# Summary Report of Research on Permanent Ground Anchor Walls, Volume IV: Conclusions and Recommendations

PUBLICATION NO. FHWA-RD-98-068

SEPTEMBER 1998

U.S. Department of Transportation
**Federal Highway Administration**

Research and Development
Turner-Fairbank Highway Research Center
6300 Georgetown Pike
McLean, VA 22101-2296

## FOREWORD

This report is part of a four-volume series which summarizes a comprehensive study on permanent ground anchor walls. Volume I (FHWA-RD-98-065) discusses current practice and limiting equilibrium analyses. Volume II (FHWA-RD-98-066) presents results of full-scale wall tests and a soil-structure interaction model. Volume III (FHWA-RD-98-067) covers model-scale wall tests and ground anchor tests. Volume IV (FHWA-RD-98-068) summarizes the first three volumes and presents conclusions and recommendations.

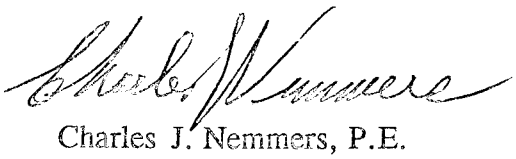

Charles J. Nemmers, P.E.
Office of Engineering
Research and Development

## NOTICE

This document is disseminated under the sponsorship of the Department of Transportation in the interest of information exchange. The United States Government assumes no liability for its contents or use thereof. This report does not constitute a standard specification or regulation.

The United States Government does not endorse products or manufacturers. Trademarks or manufacturers names appear herein only because they are considered essential to the object of this document.

# Technical Report Documentation Page

| 1. Report No. | 2. Government Accession No. | 3. Recipient's Catalog No. |
|---|---|---|
| FHWA-RD-98-068 | | PB99-163206 |

| 4. Title and Subtitle | 5. Report Date |
|---|---|
| SUMMARY REPORT OF RESEARCH ON PERMANENT GROUND ANCHOR WALLS, VOLUME IV: CONCLUSIONS AND RECOMMENDATIONS | September 1998 |
| | 6. Performing Organization Code |

| 7. Author(s) | 8. Performing Organization Report No. |
|---|---|
| Weatherby, D.E. | |

| 9. Performing Organization Name and Address | 10. Work Unit No. (TRAIS) |
|---|---|
| Schnabel Foundation Company<br>45240 Business Court, Suite 250<br>Sterling, Virginia 20166 | 3E3B0139 |
| | 11. Contract or Grant No.<br>DTFH61-89-C-00038 |

| 12. Sponsoring Agency Name and Address | 13. Type of Report and Period Covered |
|---|---|
| U.S. Department of Transportation<br>Federal Highway Administration, Research and Development<br>6300 Georgetown Pike<br>McLean, Virginia 22101-2296 | Final Report<br>September 1989–November 1997 |
| | 14. Sponsoring Agency Code |

**15. Supplemental Notes**

FHWA Contracting Officer's Technical Representative (COTR): Albert F. DiMillio, HNR-10
FHWA Technical Consultant: Richard S. Cheney, HNG-31

**16. Abstract**

Research directed toward improving the design and construction of permanent ground anchor walls is presented. The research focused on tiedback soldier beam walls for highway applications. These walls are generally less than 25 ft high, and they are supported by one or two rows of permanent ground anchors.

This volume is part of a four-volume report summarizing the research. It presents major conclusions and recommendations, research needs, and recommendations for implementing the results of the research. Recommendations for determining the shape and the magnitude of apparent earth pressure diagrams for granular soils and stiff clays, for using limiting equilibrium analyses to determine the total lateral earth load and wall stability, for estimating axial and lateral load applied to the toe, for computing the axial and lateral load-carrying capacity of the toe, for selecting the corrosion protection for the anchor tendons and the soldier beams, and for constructing and testing large-diameter ground anchors in fine-grained soils are made.

This volume is a summary of the research results reported in the first three volumes in this series. The other three volumes are entitled:

| | | |
|---|---|---|
| FHWA-RD-98-065 | Volume I | Current Practice and Limiting Equilibrium Analyses |
| FHWA-RD-98-066 | Volume II | Full-scale Wall Tests and a Soil-structure Interaction Model |
| FHWA-RD-98-067 | Volume III | Model-scale Wall Tests and Ground Anchor Tests |

In addition, a manual and computer program were developed that incorporate research results. They are entitled:

| | |
|---|---|
| FHWA-RD-97-130 | Design Manual for Permanent Ground Anchor Walls |
| FHWA-RD-98-093 | TB Wall — Anchored Wall Design and Analysis Program for Personal Computers |


| 17. Key Words | 18. Distribution Statement |
|---|---|
| Ground anchor walls, tiebacks, ground anchors, anchors, retaining walls, apparent earth pressures, earth pressures, wall deformations, ground movements, internal and external stability, limiting equilibrium, research needs | No restrictions. This document is available to the public through the National Technical Information Service, Springfield, Virginia 22161. |

| 19. Security Classif. (of this report) | 20. Security Classif. (of this page) | 21. No. of Pages | 22. Price |
|---|---|---|---|
| Unclassified | Unclassified | 89 | |

# SI* (MODERN METRIC) CONVERSION FACTORS

## APPROXIMATE CONVERSIONS TO SI UNITS

| Symbol | When You Know | Multiply By | To Find | Symbol |
|---|---|---|---|---|
| | **LENGTH** | | | |
| in | inches | 25.4 | millimeters | mm |
| ft | feet | 0.305 | meters | m |
| yd | yards | 0.914 | meters | m |
| mi | miles | 1.61 | kilometers | km |
| | **AREA** | | | |
| $in^2$ | square inches | 645.2 | square millimeters | $mm^2$ |
| $ft^2$ | square feet | 0.093 | square meters | $m^2$ |
| $yd^2$ | square yards | 0.836 | square meters | $m^2$ |
| ac | acres | 0.405 | hectares | ha |
| $mi^2$ | square miles | 2.59 | square kilometers | $km^2$ |
| | **VOLUME** | | | |
| fl oz | fluid ounces | 29.57 | milliliters | ml |
| gal | gallons | 3.785 | liters | l |
| $ft^3$ | cubic feet | 0.028 | cubic meters | $m^3$ |
| $yd^3$ | cubic yards | 0.765 | cubic meters | $m^3$ |
| NOTE: Volumes greater than 1000 l shall be shown in $m^3$. | | | | |
| | **MASS** | | | |
| oz | ounces | 28.35 | grams | g |
| lb | pounds | 0.454 | kilograms | kg |
| T | short tons (2000 lb) | 0.907 | megagrams | Mg |
| | **TEMPERATURE (exact)** | | | |
| °F | Fahrenheit temperature | 5(F-32)/9 or (F-32)/1.8 | Celcius temperature | °C |
| | **ILLUMINATION** | | | |
| fc | foot-candles | 10.76 | lux | l |
| fl | foot-Lamberts | 3.426 | candela/$m^2$ | $cd/m^2$ |
| | **FORCE and PRESSURE or STRESS** | | | |
| lbf | poundforce | 4.45 | newtons | N |
| psi | poundforce per square inch | 6.89 | kilopascals | kPa |

## APPROXIMATE CONVERSIONS FROM SI UNITS

| Symbol | When You Know | Multiply By | To Find | Symbol |
|---|---|---|---|---|
| | **LENGTH** | | | |
| mm | millimeters | 0.039 | inches | in |
| m | meters | 3.28 | feet | ft |
| m | meters | 1.09 | yards | yd |
| km | kilometers | 0.621 | miles | mi |
| | **AREA** | | | |
| $mm^2$ | square millimeters | 0.0016 | square inches | $in^2$ |
| $m^2$ | square meters | 10.764 | square feet | $ft^2$ |
| $m^2$ | square meters | 1.195 | square yards | ac |
| ha | hectares | 2.47 | acres | $mi^2$ |
| $km^2$ | square kilometers | 0.386 | square miles | |
| | **VOLUME** | | | |
| ml | milliliters | 0.034 | fluid ounces | fl oz |
| l | liters | 0.264 | gallons | gal |
| $m^3$ | cubic meters | 35.71 | cubic feet | $ft^3$ |
| $m^3$ | cubic meters | 1.307 | cubic yards | $yd^3$ |
| | **MASS** | | | |
| g | grams | 0.035 | ounces | oz |
| kg | kilograms | 2.202 | pounds | lb |
| Mg | megagrams | 1.103 | short tons (2000 lb) | T |
| | **TEMPERATURE (exact)** | | | |
| °C | Celcius temperature | 1.8C + 32 | Fahrenheit temperature | °F |
| | **ILLUMINATION** | | | |
| lx | lux | 0.0929 | foot-candles | fc |
| $cd/m^2$ | candela/$m^2$ | 0.2919 | foot-Lamberts | fl |
| | **FORCE and PRESSURE or STRESS** | | | |
| N | newtons | 0.225 | poundforce | lbf |
| kPa | kilopascals | 0.145 | poundforce per square inch | psi |

* SI is the symbol for the International System of Units. Appropriate rounding should be made to comply with Section 4 of ASTM E380.

(Revised August 1992)

# TABLE OF CONTENTS

# TABLE OF CONTENTS
*(continued)*

# LIST OF FIGURES

# LIST OF FIGURES
*(continued)*

# LIST OF FIGURES
*(continued)*

# LIST OF TABLES

# LIST OF ABBREVIATIONS AND SYMBOLS

| | | |
|---|---|---|
| AASHTO | = | American Association of State Highway and Transportation Officials |
| AEP | = | Apparent earth pressure |
| AGC | = | Association of General Contractors |
| ARTBA | = | American Road and Transportation Builders Association |
| $A_s$ | = | Surface area of soldier beam |
| $b$ | = | Soldier beam width or shaft diameter |
| $D$ | = | Toe depth |
| $d$ | = | Depth |
| $d_i$ | = | Distance when the failure wedge from two adjacent soldier beam toes intersect |
| $E_s$ | = | A secant modulus on the soil's stress-strain curve |
| FHWA | = | Federal Highway Administration |
| $F_p$ | = | Passive force |
| $F_x$ | = | Forces in the x-direction |
| $F_y$ | = | Forces in the y-direction |
| $H$ | = | Excavation depth or height |
| $h$ | = | Height of wall |
| $h_1$ | = | Depth of excavation to allow the installation of the upper ground anchor |
| $K$ | = | A reduction factor to apply to $s_u$ to give the adhesion between the soldier beam and the clay |
| $K_A$, $K_a$ | = | Coefficient of active earth pressure |
| $K_o$ | = | Coefficient of at-rest earth pressure |
| $K_p$ | = | Coefficient of passive earth pressure |

# LIST OF ABBREVIATIONS AND SYMBOLS
*(continued)*

| | | |
|---|---|---|
| $K_{reqd}$ | = | Required earth pressure coefficient |
| $L$ | = | Span distance |
| NCHRP | = | National Cooperative Highway Research Program |
| $P_p$ | = | Passive resistance from the soil |
| $P_{reqd}$ | = | External force required for stability |
| PTI | = | Post Tensioning Institute |
| $p$ | = | Unit load |
| pcf | = | Pounds per cubic foot |
| psf | = | Pounds per square foot |
| $p_{active}$ | = | Active earth pressure below the bottom of the excavation |
| $p_{AEP}$ | = | Apparent earth pressure |
| $R$ | = | Reaction vector in a force polygon |
| $R_a$-$y$ curve | = | Curve that describes the load and deflection relationship for the active side of the toe of a soil-soldier beam system |
| $R_p$-$y$ curve | = | Curve that describes the load and deflection relationship for the passive side of the toe of a soil-soldier beam system |
| $S_{cr}$ | = | Spacing between two soldier beams where the passive resistance at the toe changes from single soldier beam behavior to group behavior |
| $SP_h$ | = | Horizontal resistance from the wall below the failure surface |
| $Sp_v$ | = | Vertical resistance from the wall below the failure surface |
| $s$ | = | Soldier beam spacing |
| $s_c$ | = | Clear spacing between soldier beams |
| $s_u$ | = | Undrained shear strength |
| $T$ | = | Ground anchor load |

# LIST OF ABBREVIATIONS AND SYMBOLS
*(continued)*

| | | |
|---|---|---|
| tsf | = | Tons per square foot |
| *T-y* curve | = | Curve that describes the load elongation behavior of a ground anchor |
| $W$ | = | Weight vector in a force polygon |
| $y_b$ | = | Bulging deformations |
| $y_c$ | = | Cantilever deformation |
| $\alpha$ | = | Anchor inclination |
| $\alpha$ | = | Angle of the failure plane with respect to the horizontal |
| $\alpha$ | = | Angle that defines the shape of a failure wedge for the toe of a soldier beam in sand |
| $\gamma$ | = | Total unit weight |
| $\gamma_{ave}$ | = | Average total unit weight |
| $\delta$ | = | Angle of friction between soil and soldier beam or wall |
| $\theta$ | = | Angle that defines the shape of a failure wedge for the toe of a soldier beam in clay |
| $\xi$ | = | Ratio of the depth of the internal stability failure surface below the bottom of the excavation to the final depth of excavation |
| $\sigma'$ | = | Effective normal stress |
| $\sigma_v'$ | = | Effective overburden pressure |
| $\phi$ | = | Angle of internal friction, friction angle |
| $\phi_{mob}$ | = | Mobilized friction angle |

# CHAPTER 1
# INTRODUCTION

Permanent ground anchor wall systems, often called tiedback walls, use tensile elements anchored in the ground to support earth retaining structures or stabilize landslides. These walls are built in excavated cuts from the top down. For most highway applications, ground anchor walls consist of anchored soldier beams with temporary wood lagging and a permanent cast-in-place concrete face. Figure 1 shows a typical anchored wall and the major components of the wall. Soldier beams distribute the ground anchor load to the ground and support the earth at the face of the cut. The components of a ground anchor are shown in Figure 2.

The steps involved in constructing a permanently anchored soldier beam wall are shown in Figure 3. First the soldier beams are driven or drilled into the ground from the existing ground surface. After the soldier beams are installed, the excavation proceeds to the first ground anchor level. As the excavation is made, wood lagging or shotcrete is applied to support the ground between the soldier beams temporarily. Next, the ground anchors are installed. They are made by driving or drilling a hole into the ground behind the wall. After the hole has reached the desired depth, a prestressing steel tendon is grouted into the ground. The grouted anchor fixes the tendon to the ground at the far end. After the cement grout has cured, the ground anchor is load tested and locked-off to the soldier beam. Then the excavation and placement of lagging or shotcrete continues to the next anchor level or the bottom of the cut. If additional levels of ground anchors are required, the steps described above are repeated.

After the excavation is completed, prefabricated drains are attached to the lagging or shotcrete. An unreinforced concrete leveling pad is often cast at the bottom of the wall. The pad enables the wall forms to be easily set and it is not designed. A permanent, reinforced, cast-in-place concrete face is constructed from the bottom up. Headed studs are used to attach the concrete face to steel soldier beams. Grouted or epoxied dowels are used with drilled-in, reinforced concrete soldier beams.

Driven steel sheet piling, soldier beams in a deep soil mixed trench or structural diaphragm walls are occasionally used for anchored walls. These walls are built when it is necessary to cut off groundwater from behind or under the wall. Sheet piling or deep soil mixed walls have been used when the ground between soldier beams will not support itself long enough to install lagging or shotcrete.

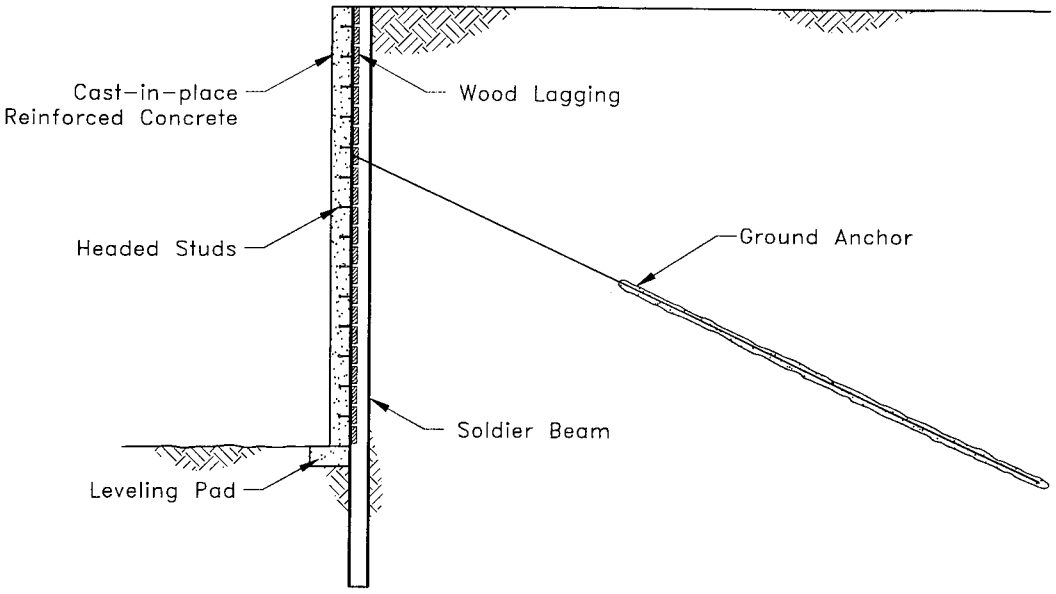


**FIGURE 1**
**Permanent Ground Anchor Retaining Wall**

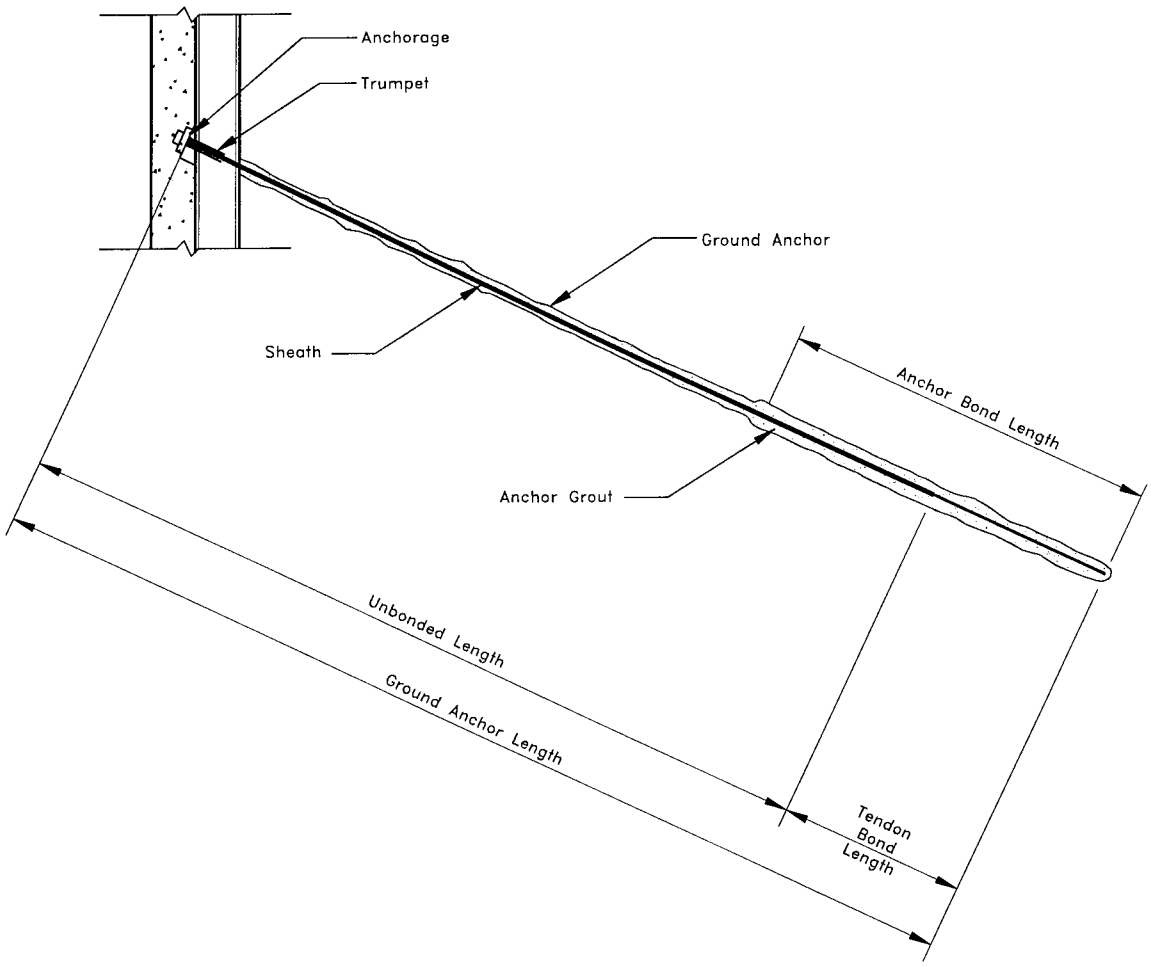


**FIGURE 2**
**Ground Anchor Components**

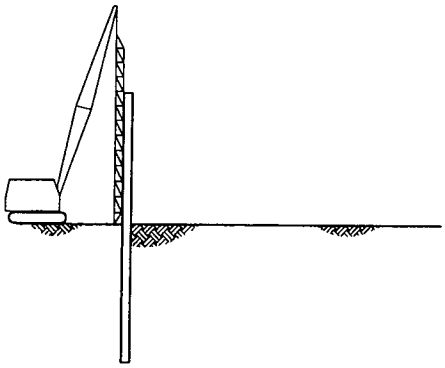

a) Install soldier beam

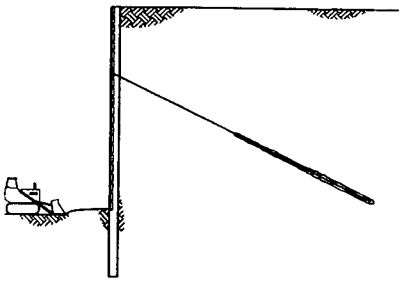

d) Complete excavation

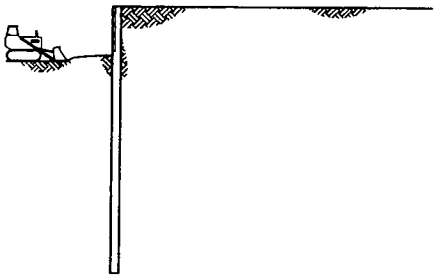

b) Excavate

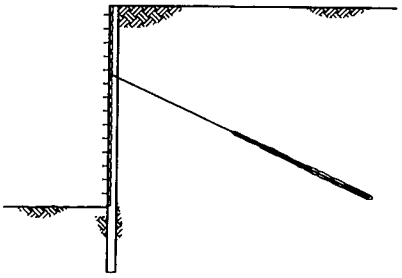

e) Install headed studs and prefabricated drainage

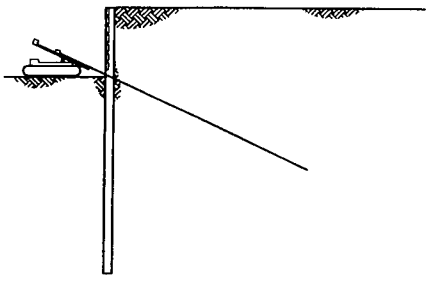

c) Install ground anchor

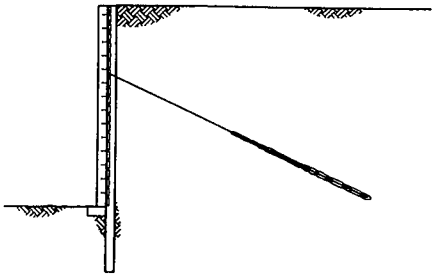

f) Pour cast-in-place facing

**FIGURE 3**
**Construction Steps for Ground Anchor Wall**

Permanent ground anchor walls have been routinely built in the private sector since the late 1970's. A considerable base of empirical knowledge exists with respect to their design, construction and performance. Public agencies have built many permanently anchored retaining walls since the 1980's. Most walls in the public sector were designed using conservative guidelines adopted in the 1980's. In the late 1980's, the Federal Highway Administration (FHWA) recognized that the design guidelines could be improved. It funded a research program to improve the understanding of the behavior of permanent ground anchor walls and to develop a design manual for highway walls.

The research program was directed toward ground anchor walls constructed using tiedback soldier beams. For highway applications, these walls are generally less than 25 ft high, and they are supported by one or two rows of permanent ground anchors.

This volume is part of a four-volume report summarizing the research. It presents major conclusions and recommendations, research needs, and recommendations for implementing the results of the research. The chapters in Volume IV include the following:

- Chapter 2 presents recommendations for determining the magnitude and shape of apparent earth pressure diagrams for granular soils and stiff clays, using limiting equilibrium analyses to determine total lateral load and wall stability, estimating the axial and lateral load applied to the soldier beam toe, computing the axial and lateral load-carrying capacity of the soldier beam toe, selecting the corrosion protection for ground anchor tendons and soldier beams, and constructing and testing large-diameter ground anchors in fine-grained soils. Observations regarding wall and ground movements also are included.
- Chapter 3 presents research needs identified during the performance of the work under this contract.
- Chapter 4 provides recommendations for implementing the results of the research.

The other three volumes of the research report are entitled:

| | |
|---|---|
| Volume I | Current Practice and Limiting Equilibrium Analyses (Long, et al., 1998) |
| Volume II | Full-scale Wall Tests and a Soil-structure Interaction Model (Weatherby, et al., 1998) |
| Volume III | Model-scale Wall Tests and Ground Anchor Tests (Mueller, et al., 1998) |

The four volumes address the major elements of permanent ground anchor wall design and provide guidance and recommendations to be used in the development of a design procedure presented in a separate manual. Some research finds were incorporated in a computer code developed for the design or analysis of permanent ground anchor walls. The manual is entitled, *Design Manual for Permanent Ground Anchor Walls* (Weatherby, 1997), and the computer program is called *TB Wall — Anchored Wall Design and Analysis Program for Personal Computers* (Urzua and Weatherby, 1998).

Recommendations presented in this report are intended to apply to permanent ground anchor walls for typical highway applications. They were not developed for temporary earth support systems, but many principles presented apply to both permanent and temporary construction.

# CHAPTER 2
# CONCLUSIONS AND RECOMMENDATIONS

Recommendations in this chapter are based on research performed on two full-scale wall sections, four large-scale model walls, 10 large-diameter ground anchors installed in a fine-grained soil, analytical studies and experience (Long, et al., 1998; Weatherby, et al., 1998; and Mueller, et al., 1998). They were incorporated in a design procedure for permanent tiedback soldier beam walls for highway applications.

## 2.1 EARTH PRESSURES

**Design permanent ground anchor walls to support lateral loads given by apparent earth pressure diagrams.** The magnitude and shape of the diagrams are based on measured strut loads, limiting equilibrium analyses, experience, and an understanding of anchored wall behavior. **These diagrams are suitable for walls supported by one or multiple rows of anchors. Consider the soil at the bottom of the excavation to be a strut and the soldier beam to be hinged at the bottom of the excavation when determining bending moments using earth pressure diagrams for granular soils, stiff clays, and soft to medium clays with a firm stratum near the bottom of the excavation.** When soft to medium clay extends below the bottom of the excavation to great depth, then the soldier beam is designed to cantilever around the lowest support.

### 2.1.1 Development of Apparent Earth Pressure Diagrams

Apparent earth pressure (AEP) diagrams or envelopes were originally developed to give the magnitude and distribution of earth pressures on braced excavation support systems. They were derived by measuring strut load increases on braced excavations as the excavation deepened. Little displacement was required for the stiff struts to pick up load.

Experience with strutted walls in the last 100 years has shown that the total lateral force measured on the walls is close to values calculated from active earth pressure theory. However, the distribution of earth pressure on strutted walls does not fit the classical theories of Coulomb and Rankine. Instead of earth pressure increasing linearly with depth (triangular distribution), it has long been observed that high pressures develop in the upper part of the wall, as the supports are placed. The upper supports restrain the wall from rotating outward sufficiently to reduce the earth pressures to active (triangular distribution).

Field measurements of strut loads on internally braced excavations in sands (principally in Berlin, Munich, and New York City) and in clays (principally in Chicago) led to development of the apparent earth pressure envelopes (Terzaghi and Peck, 1967) currently used. Apparent earth pressures were calculated by dividing measured strut loads by the area of the wall supported by each strut. Soil at the bottom of the cut was considered a strut, and the beam was

hinged at the bottom of the excavation. The pressures were not directly measured, thus the name apparent earth pressures. Pressure distributions varied depending on the details of construction. For example, higher loads developed in some struts because they were more highly pre-loaded, or because they were installed quickly after excavating.

Apparent earth pressure diagrams were developed to be envelopes that encompassed the highest apparent earth pressures determined from the measured strut loads and, thus, predicted greater pressures than those calculated from most of the struts. Accordingly, the total load from an apparent earth pressure diagram was greater than the total measured earth load. Apparent earth pressure envelopes are rectangular or trapezoidal in shape. Typical apparent earth pressure diagrams used today are presented in Figure 4. These diagrams are discussed by Terzaghi, et al. (1996) and Schnabel (1982). An important assumption in the use of these diagrams is that the static water level is below the base of the excavation.

The apparent earth pressure envelope for sand (Figure 4a) is a rectangle with an apparent earth pressure ($p_{AEP}$) equal to

$$p_{AEP} = 0.65 K_A \gamma H \quad \ldots [2.1]$$

where $K_A$ is the Rankine active earth pressure coefficient ($K_A = \tan^2\{45-\phi/2\}$), $\gamma$ is the total unit weight of the soil, and $H$ is the height of the cut. Applying the apparent earth pressure along the full height of the cut produces a total lateral force that is 1.3 times the value predicted from Rankine active earth pressure theory.

Figure 4b is the apparent earth pressure envelope for soft to medium clays. The maximum apparent earth pressure for a soft to medium clay is expressed as

$$p_{AEP} = K_A \gamma H \quad \ldots [2.2]$$

where $K_A = 1\text{-}4 s_u / \gamma H$, $\gamma$ is the total unit weight of the soil, $H$ is the height of the cut, and $s_u$ is the undrained shear strength of the soil. Soft to medium clays have a ratio of $\gamma H / s_u$ greater than about six. The distribution of apparent earth pressure varies from zero to full pressure at a depth of $0.25H$ (Figure 4b). The pressure remains constant below a depth of $0.25H$. Applying the apparent earth pressure along the full height of the cut produces a total lateral force that is 1.75 times the value that would be predicted from active earth pressure theory. When the soft to medium clay extends well below the bottom of the excavation, the value of $K_A$ is determined using recommendations developed by Henkel (1971).

The apparent earth pressure distribution for stiff-fissured clays is shown in Figure 4c. The maximum apparent earth pressure for a stiff clay ranges from

$$p_{AEP} = 0.2\gamma H \text{ to } 0.4\gamma H \quad \ldots [2.3]$$

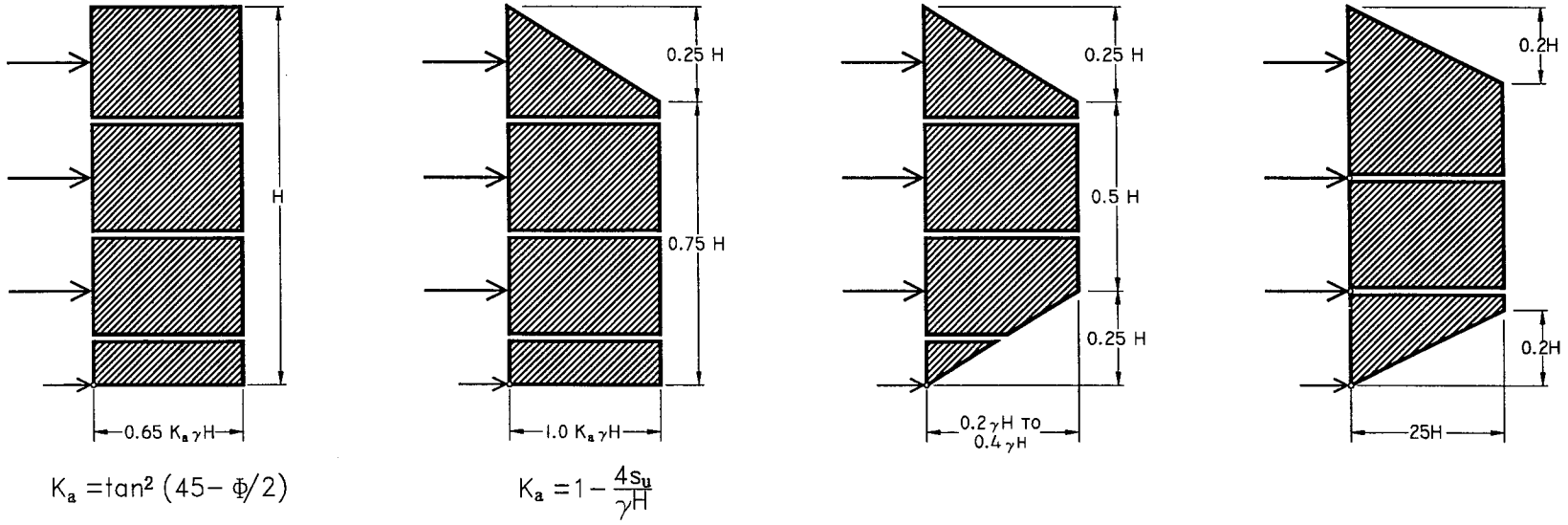


**FIGURE 4**
**Apparent Earth Pressure Diagrams**

Stiff clays are identified as those with ratios of $\gamma H/s_u$ less than four. When $\gamma H/s_u$ is equal to four, $K_A$ is zero, and the active earth pressure is zero. Significant loads were measured on struts supporting walls in stiff clay. These loads did not develop from a state of limiting equilibrium. Instead, the stresses and the deformations behind a wall in stiff clay correspond to a quasi elastic state (Terzaghi, et al., 1996). In a quasi elastic state, the earth pressures depend on the at-rest pressures, the in situ modulus of elasticity, the stiffness of the supports, the depth of over-excavation before each level of support is installed, and the pre-load applied to the supports.

The total lateral earth load for cuts in clay having values of $\gamma H/s_u$ between four and six are determined using both the soft to medium clay (Figure 4b and Equation 2.2)and the stiff clay (Figure 4c and Equation 2.3) diagram. The apparent earth pressure diagram that produces the greatest total earth load is used for design.

Terzaghi and Peck apparent earth pressure diagrams (Figures 4a to 4c) assume that the wall is either in sand or clay. Frequently, excavation support systems and anchored walls are built in mixed grounds. In mixed grounds, selecting the appropriate Terzaghi and Peck apparent earth pressure diagram and estimating the intensity of the earth pressure is difficult. For more than 35 years, Schnabel Foundation Company has successfully used a single apparent earth pressure diagram to design excavation support systems and permanent ground anchored retaining walls in sands, stiff clays, and mixed grounds. Figure 4d shows the $25H$ trapezoidal apparent earth pressure diagram recommended by Schnabel (1982). The total lateral earth load estimated using Schnabel's diagram is approximately equal to the load determined using Terzaghi and Peck's diagram for a sand with an angle of friction of 35° or their diagram for a stiff clay with the pressure equal to $0.2\gamma H$. Measured strut loads in sands and stiff clays fit within the $25H$ envelope. This diagram is not appropriate for walls in low-strength cohesive soils, and the intensity of the pressure may be increased for fissured, heavily overconsolidated clays.

**Apparent earth pressure diagrams developed from strut measurements are used to design permanent ground anchor walls. Implicit in the use of these diagrams is that the groundwater level remains below the bottom of the wall. Ground anchors, which are much more flexible than struts, are tensioned to loads near their design load to reduce lateral wall movements during excavation. Load cell measurements show that ground anchor loads do not change significantly during excavation. Measured ground anchor loads reflect the pre-load (lock-off load) rather than the load imposed by the ground during construction (as observed with strutted excavations).**

### 2.1.2 Anchor Loads and Soldier Beam Bending Moments

Figure 5 shows the two common methods used to calculated ground anchor loads and soldier beam bending moments from apparent earth pressure diagrams. **Loads are determined by either the tributary area method or by dividing the beam into simple beams.** Bending moments in the soldier beam down to the first ground anchor are calculated by summing moments around the upper anchor. **Below the upper ground anchor, the design methods**

**conservatively predict the magnitudes of the maximum bending moments, but they do not predict their locations** (Weatherby, et al., 1998).

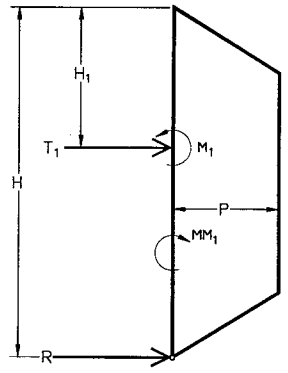


*a) Single-tier walls*

$T_1$ = Σmom. @ R

R = Tot. Earth Pressure−$T_1$

$M_1$ = Σmom. @ $T_1$

$MM_1$ = Max. moment where shear is zero

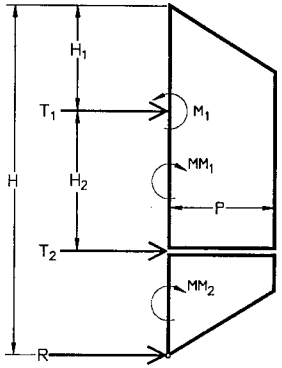


*b) Multi-tier walls (simple beams)*

$T_1$ = Σmom. @ $T_2$

$T_2$ = Σmom. @ R

R = Tot. Earth Pressure−$T_1$ −$T_2$

$M_1$ = Σmom. @ $T_1$

Max. moment below $T_1$ = larger of $MM_1$ or $MM_2$

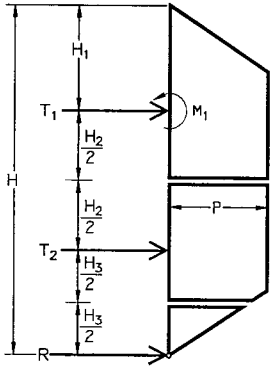


*c) Multi-tier walls (tributary areas)*

$T_1$ = Load over span $H_1 + \frac{H_2}{2}$

$T_2$ = Load over span $\frac{H_2}{2} + \frac{H_3}{2}$

R = Load over span $\frac{H_3}{2}$

$M_1$ = Σmom. @ $T_1$

Max. moment below $T_1$ = $\frac{1}{10} pL^2$ (L= larger of $H_2$ or $H_3$)

(Moments below $T_1$ often reduced)

**FIGURE 5**
**Procedures for Determining Anchor Loads and Soldier Beam Moments from Apparent Earth Pressure Diagrams**

### 2.1.3 The Shape of the Apparent Earth Pressure Diagram

Research, experience, and observations indicate:

- **The shape of the apparent earth pressure diagrams depends upon the location of the supports** (Weatherby, et al., 1998).
- **Soldier beams distribute the support loads to the ground and concentrate the pressures at the support locations** (Mueller, et al., 1998, and Weatherby, et al., 1998).
- **Earth pressures in granular soils are zero at the ground surface.**
- **Trapezoidal apparent earth pressure diagrams predict the earth pressures in stiff, fine-grained soils.**

These observations led to the development of a modified trapezoidal apparent earth pressure diagram for granular soils and stiff clays.

Figure 6 illustrates how the shape of the modified trapezoidal apparent earth pressure diagram changes to fit the locations of the supports for the one- and two-tier wall sections in the full-scale test wall. Both diagrams in Figure 6 have a total lateral load of 100 kips. The 100-kip load was the total load from the design pressure diagram ($25H$ trapezoid) for both sections of the 25-ft high test wall built in a medium-dense sand.

Earth pressures in the diagrams shown in Figure 6 increase to a maximum at a depth equal to two-thirds the distance to the upper ground anchor. For a wall supported by one row of anchors, the maximum pressure continues downward for a distance equal to one-third the height of the wall. Below that depth, the pressure decreases linearly to zero at the bottom of the excavation. For a wall supported by two or more rows of ground anchors, the maximum earth pressure continues to a point below the lowest support equal to one-third the distance from the lowest support to the bottom of the excavation. From there the pressure decreases linearly to zero at the bottom of the excavation. The total load in both earth pressure diagrams is the same, but the intensity of the pressure changes with changes in the shape of the diagram.

Figure 7 shows the design bending moment diagram, the bending moment diagram from the new apparent earth pressure diagram, and the average measured bending moments in two soldier beams in the one-tier section of the full-scale test wall. Bending moments were computed assuming a hinge at the bottom of the excavation. The figure shows that the bending moments predicted from the new apparent earth pressure diagram matched the measured bending moments slightly better than the moments from the design diagram. Table 1 gives the actual ground anchor load, the design ground anchor load, and the anchor load from the new diagram. The actual anchor load in Table 1 is less than the loads determined from the apparent earth pressure diagrams because the anchors were locked-off at a load equal to 75 percent of the design load. Table 1 show that both diagrams give reasonable ground anchor load predictions.

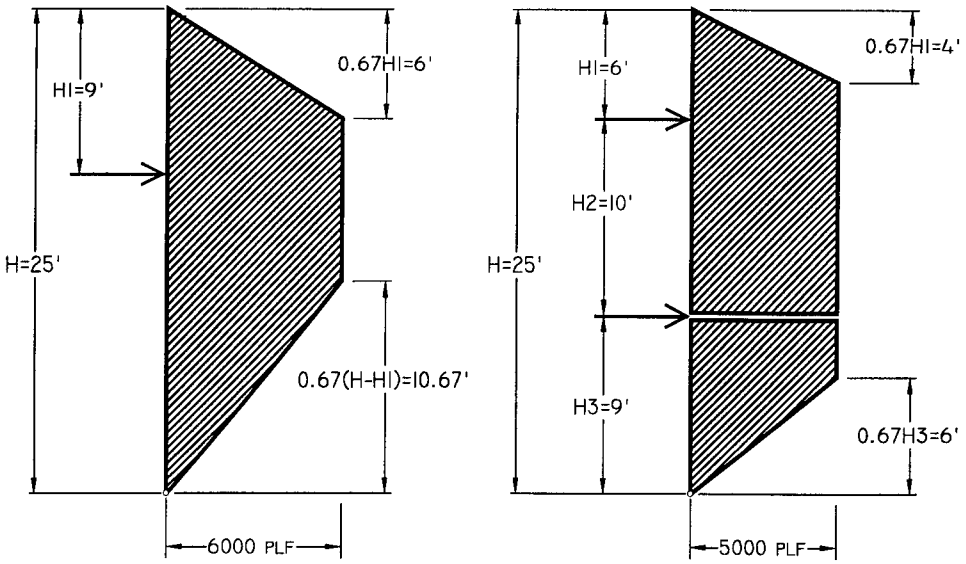


a) One-tier wall

b) Two-tier wall

**FIGURE 6**
**Modified Trapezoidal Apparent Earth Pressure Diagram for the One- and Two-tier Wall Sections in the Full-scale Test Wall (shape determined by anchor locations)**

**TABLE 1**
**Comparison of the Average Horizontal Component of the Ground Anchor Load for Two Soldier Beams in the One-tier Wall Section with the Design Anchor Load and the Anchor Load Predicted Using the Modified Trapezoidal Apparent Earth Pressure Diagram**

| | ANCHOR LOAD (kips) |
|---|---|
| Actual | 62.69 |
| Design Pressure Diagram | 78.12 |
| New Apparent Earth Pressure Diagram | 84.20 |

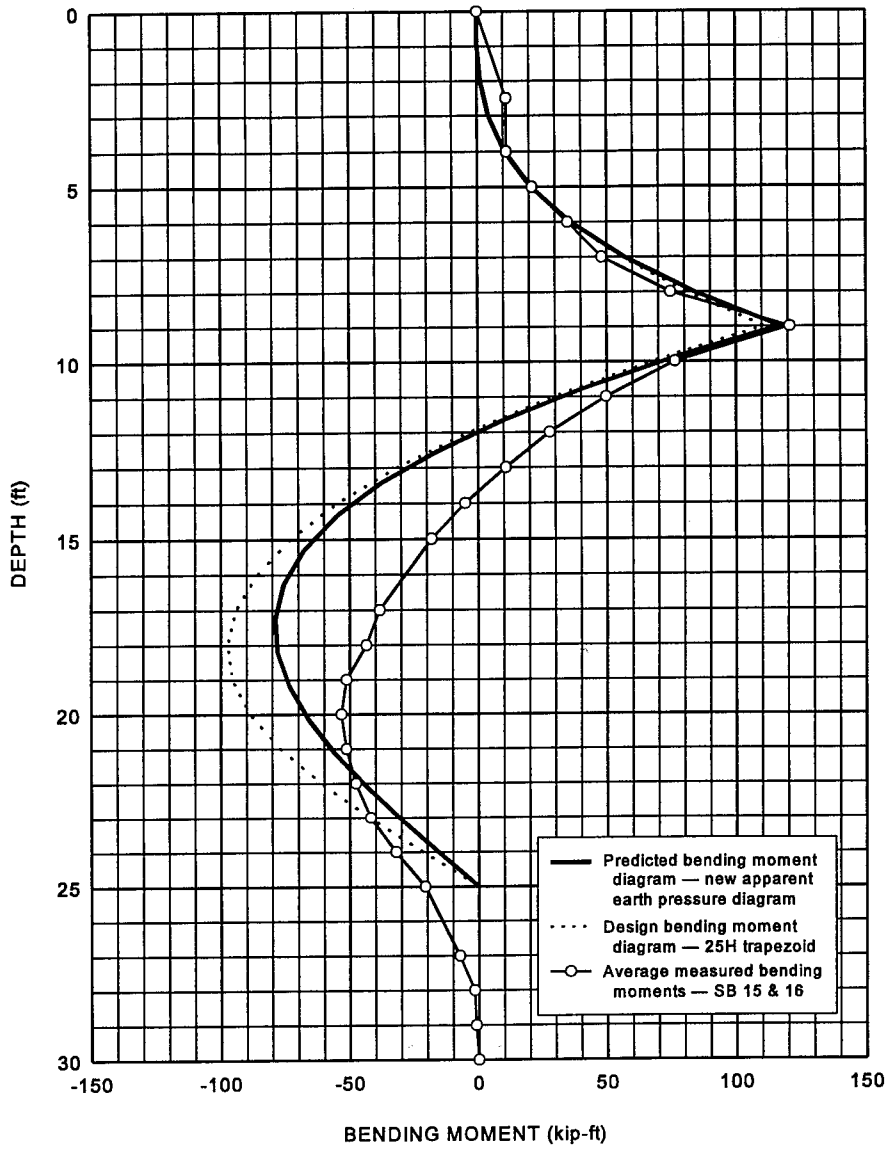


**FIGURE 7**
**Comparison of the Average Bending Moments in Two Soldier Beams in the One-tier Wall Section with the Design Moment Diagram and the Moment Diagram Predicted Using the Modified Trapezoidal Apparent Earth Pressure Diagram**

Figure 8 shows the design bending moment diagram, the bending moment diagram for the new apparent earth pressure diagram, and the average measured bending moments for two soldier beams in the two-tier section of the full-scale test wall. Table 2 gives the actual ground anchor loads, the design ground anchor loads, and the anchor loads from the new apparent earth pressure diagram. Bending moment diagrams and anchor loads were developed using the hinge method. Figure 8 shows that the new apparent earth pressure diagram predicts a higher bending moment at the upper ground anchor than the design pressure diagram (25*H* trapezoid).

The predicted bending moment at the upper ground anchor was 43.33 kip-ft for the new diagram and 35.83 kip-ft for the design diagram (25*H* trapezoid). The maximum predicted bending moment below the upper anchor was 42.66 kip-ft for the new pressure diagram compared with 45.66 kip-ft for the design pressure diagram (25*H* trapezoid). Bending moments predicted using the modified apparent earth pressure diagram were closer to the measured moments than the design moments. Table 2 shows that both apparent earth pressure diagrams predicted reasonable ground anchor loads.

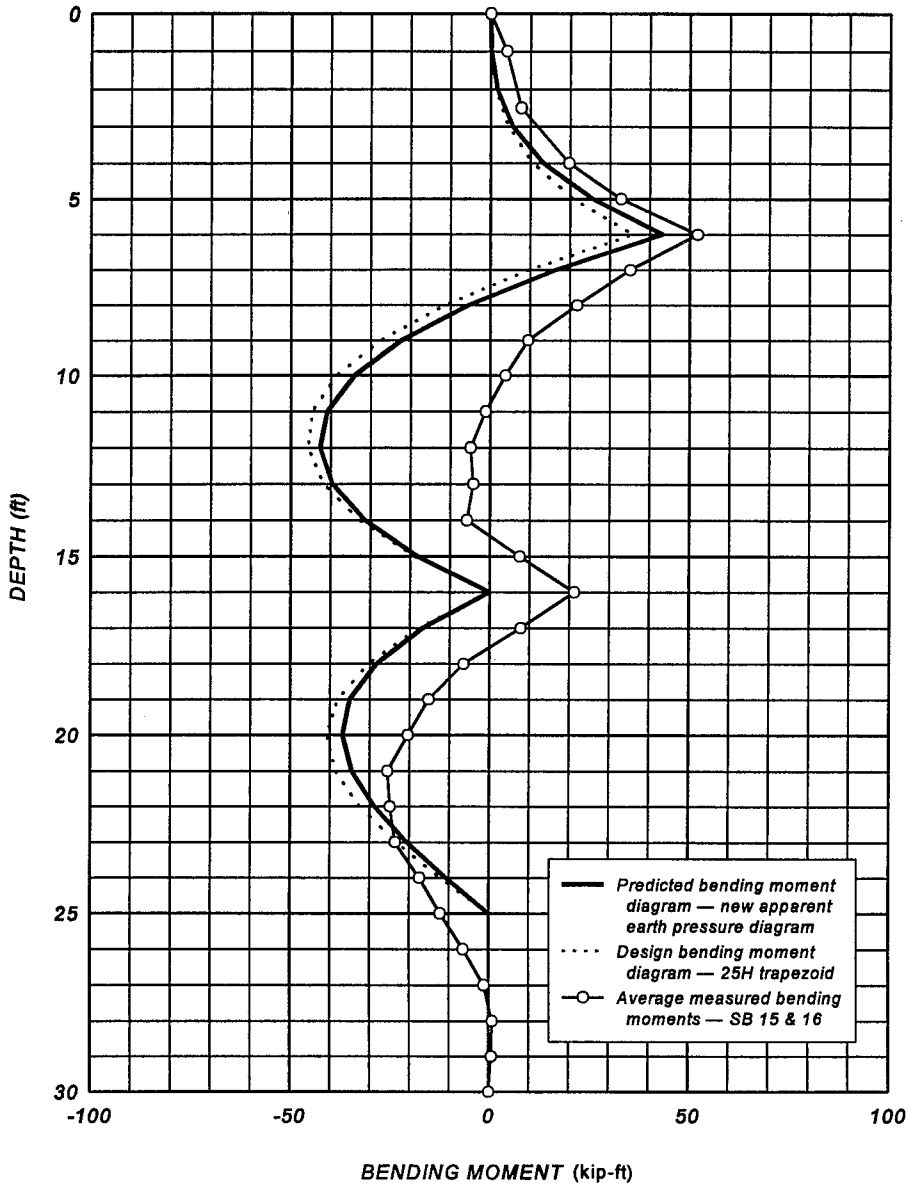


**FIGURE 8**
**Comparison of the Average Bending Moments in Two Soldier Beams in the Two-tier Wall Section with the Design Moment Diagram and the Moment Diagram Predicted Using the Modified Trapezoidal Apparent Earth Pressure Diagram**

**TABLE 2**
**Comparison of the Average Horizontal Component of the Ground Anchor Loads for Two Soldier Beams in the Two-tier Wall Section with the Design Anchor Loads and the Anchor Loads Predicted Using the Modified Trapezoidal Apparent Earth Pressure Diagram**

| | ANCHOR LOAD (kips) | |
|---|---|---|
| | Upper Anchor | Lower Anchor |
| Actual | 35.40 | 25.56 |
| Design Pressure Diagram | 46.08 | 41.60 |
| New Apparent Earth Pressure Diagram | 49.33 | 39.84 |

Figures 7 and 8 show that **apparent earth pressure diagrams should be used when designing one- and two-tier walls. In granular soils and stiff ground, assume a hinge and a strut at the bottom of the excavation.** Model tests results presented by Mueller, et al. (1998) confirmed this conclusion. Mueller reported that the model walls had to translate $0.014H$ before the earth pressure distribution changed from a trapezoidal distribution and approached a triangular distribution. This would correspond to 4.5 in of translational movement for a 25-ft high wall. Movements of this amount are 5 to 10 times larger than those observed in the field.

### 2.1.4 Determining Total Lateral Support Loads Using Limiting Equilibrium Methods

**Apparent earth pressure diagrams for sand and soft to medium clays relate measured loads to loads determined using limiting equilibrium analyses** (Terzaghi, et al., 1996, and Long, et al., 1998). Limiting equilibrium methods use simple free-body diagrams or general purpose slope stability computer programs to calculate the total lateral earth load that must be supported by the ground anchors and the toe. **The total lateral load from Terzaghi and Peck's sand or soft to medium clay apparent earth pressure diagrams are equal to the total lateral loads determined using limiting equilibrium analyses with a factor of safety of about 1.3 on the shear strength** (Long, et al., 1998). Therefore, **a factor of safety of 1.3 on the shear strength of the soil is recommended when using limiting equilibrium methods to determine the total lateral support loads for the design of anchored walls and landslide stabilization walls.** A force equilibrium method and a general purpose slope stability program are used to illustrate how limiting equilibrium methods can be used to determine the total lateral earth load.

#### 2.1.4.1 Force Equilibrium Method

Free-body and force diagrams for the force equilibrium method are shown in Figure 9. The anchored wall system retains a vertical cut in a sand with frictional strength, $\phi$, average total

unit weight, $\gamma$, and height, $H$. The unbonded length of the anchor extends far behind the wall to ensure that the critical failure surface passes above the anchor zone and the full anchor load contributes to wall stability. The potential failure plane passes through the toe of the wall at depth, $d$, and mobilizes a passive resistance from the soil, $P_p$, and a horizontal and vertical resistance from the wall below the failure surface ($SP_h$, $SP_v$, respectively). $SP_h$ will be the smaller of the shear strength of the wall or the lateral resistance of the wall below the failure surface.

For simplicity, the shape of the failure surface is assumed to be a straight line (BC). Beneath the bottom of the cut, the failure surface is assumed to be shaped as a log spiral on the passive side. For soldier beam and lagging walls, significant soil to soil contact exists, thus interface resistance along the vertical face CE is assumed to be equal to the strength of the soil. Passive resistance above the failure surface is $P_p = \frac{1}{2}K_p\gamma d^2$, where $\gamma$ is the total unit weight. Passive earth pressure coefficients assuming a log-spiral failure surface (Figure 10) are used (Terzaghi, et al., 1996).

The contribution of forces from the anchor and soldier beam are shown as force vectors $T$, $SP_h$, and $SP_v$ in Figure 9c. For simplicity and for ease of comparison with apparent earth pressure diagrams and the general purpose slope stability computer programs, the three forces are treated as a horizontal force with magnitude $P_{reqd}$. A wall of unit width is assumed. Thus, $P_{reqd}$ represents the horizontal force required to provide stability to the vertical cut per unit width. Taking $P_{reqd}$ as horizontal implicitly assumes that the vertical force in the soldier beam ($SP_v$) is equal in magnitude (and opposite in direction) to the vertical component of the anchor load ($T \cdot \sin(i)$). In addition, the groundwater table is well below the bottom of cut, and the soil has the same shear strength and unit weight throughout the profile. This allows the forces acting on the soil to be considered in the equilibrium equations (Figure 11).

The solution for the external force required for stability ($P_{reqd}$) continues by summing the forces in the x-direction to get:

$$\Sigma F_x = P_p \cos(\delta) + P_{reqd} - R \sin(\alpha - \phi) \quad \ldots [2.4]$$

and summing forces in the y-direction (vertical) to get:

$$\Sigma F_y = W - P_p \sin(\delta) - R \cos(\alpha - \phi) \quad \ldots [2.5]$$

Combining the two equations and solving for $P_{reqd}$ results in the following expression:

$$P_{reqd} = \frac{1}{2}\gamma H^2 \left[ \frac{(1+\xi)^2}{\tan(\alpha)} - K_p \xi^2 \left( \sin(\delta) + \frac{\cos(\delta)}{\tan(\alpha - \phi)} \right) \right] \tan(\alpha - \phi) \quad \ldots [2.6]$$

where $\xi$ is the ratio of $d/H$, $\alpha$ is the angle of the failure plane with respect to the horizontal (all other parameters have been defined previously). The solution proceeds by varying values of $\xi$ and $\alpha$ until a maximum for $P_{reqd}$ is determined. Values of $P_{reqd}$ are for a factor of safety

of 1.0. Solutions for Equation 2.6 for soil friction angles of 20°, 30°, and 40° are presented in Table 3 in non-dimensional form as $K_{reqd} = P_{reqd} / (\frac{1}{2}\gamma H^2)$.

Thus, the total load required to support a vertical cut of height $H$, is $P_{reqd} = \frac{1}{2}\gamma H^2 K_{reqd}$ with a factor of safety of 1.0.

Solutions for Equation 2.6 include failure surfaces that pass below the bottom of the cut (base failures). This explains why $K_{reqd}$ for a soil with a friction angle of 30° is about 4 percent greater than the Rankine active earth pressure coefficient. Rankine failure surfaces go through the bottom corner of the cut. For soils with a friction angle less than 30°, the difference between the Rankine active earth pressure coefficient and $K_{reqd}$ increases since the failure surface drops farther below the bottom of the cut.

**TABLE 3**
**Magnitudes of $K_{reqd}$ for the Force Equilibrium Method (base failure)**

| $\phi$ (deg) | $K_{reqd}$ | $\xi$ | $\alpha$ |
|---|---|---|---|
| 20 | 0.570 | 0.162 | 54 |
| 30 | 0.349 | 0.047 | 60 |
| 40 | 0.220 | 0.012 | 65 |

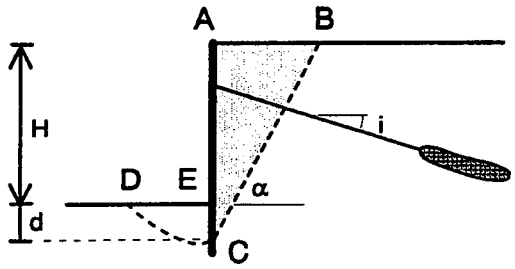


a) Example of a tiedback wall system

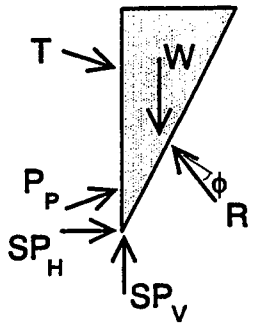


b) Free-body diagram

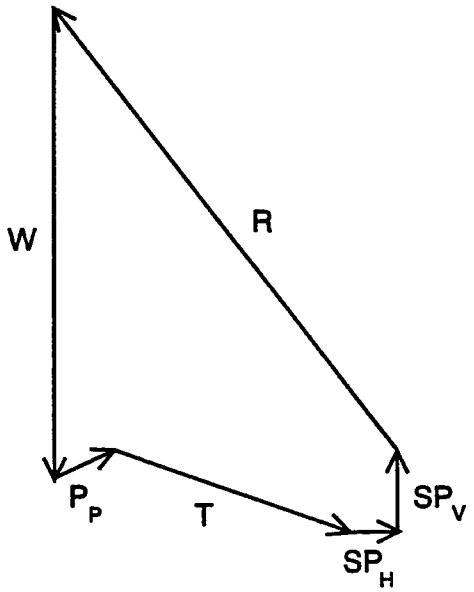


c) Force vectors acting on area ABCE

**FIGURE 9**
**Free-body and Force Diagrams for the Force Equilibrium Method for an Anchored Wall**

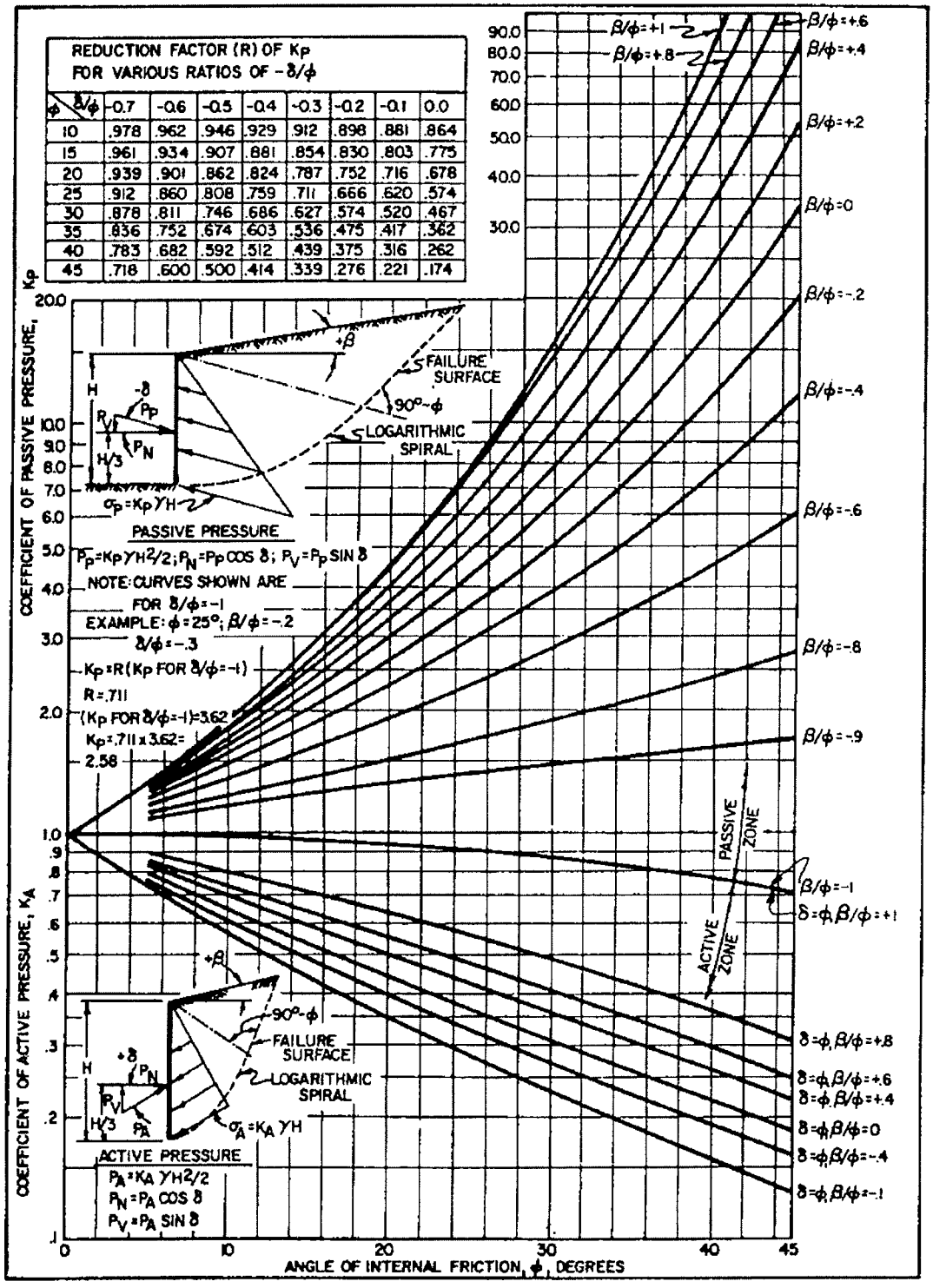


**FIGURE 10**
**Passive Earth Pressure Coefficients**
**(Department of the Navy, 1982)**

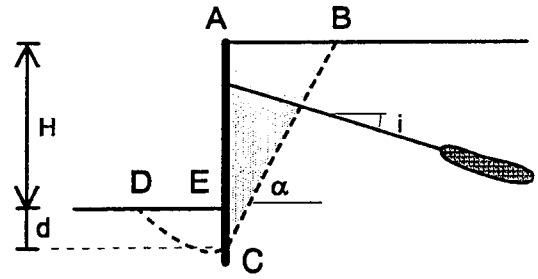


a) Example of a tiedback wall system

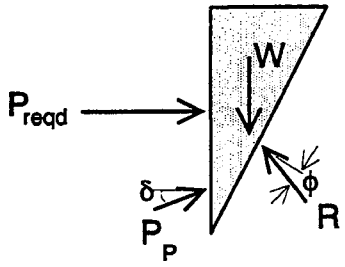


b) Free-body diagram

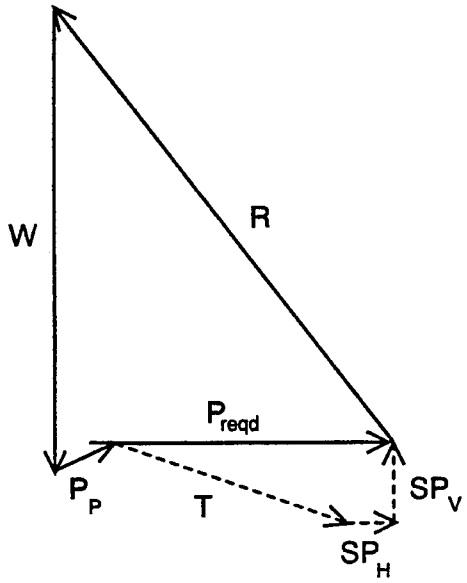


c) Force vectors acting on area ABCE

**FIGURE 11**
**Force Equilibrium Method for an Anchored Wall with $P_{reqd}$**

2.1.4.2 Slope Stability Computer Analysis

General purpose slope stability computer programs can be used to determine the total lateral earth load for the design of temporary and permanent ground anchor walls. These programs allow complicated surcharge loads, groundwater, and layered soil deposits to be modeled. They also can model ground whose shear strength is developed from both frictional resistance and cohesion. However, **many general purpose slope stability computer programs are unable to model the ground anchors as concentrated loads on the face of the wall. Apparently, they do not distribute the concentrated ground anchor loads properly throughout the slices to the failure surface.**

**Many computer programs can be used for ground anchor wall design by applying a horizontal surcharge load to the face of the wall. The surcharge load is directed toward the ground being supported. To distinguish the wall from a vertical slice, and the surcharge load from an interslice force, the wall is battered slightly (usually 1 ft).** Figure 12 shows the graphical output from a STABL5M (Achilleos, E., 1988) analysis where a horizontal surcharge load equivalent to a total lateral earth load of 23,800 lb was applied to the wall, giving a factor of safety of 1.3. In the analysis the soil was assumed to have a friction angle of 30° and a unit weight of 115 pcf. A horizontal surcharge load was used so the load could be compared with that developed from the force equilibrium method and Terzaghi and Peck's sand diagram.

Table 4 compares the total lateral earth load computed using the force equilibrium method, STABL5M, and Terzaghi and Peck's apparent earth pressure diagram. Each analysis assumed a 30-ft-high wall, a soil friction angle of 30°, and a soil unit weight of 115 pcf. A factor of safety of 1.3 was applied to the shear strength when computing the load using the force equilibrium method and the computer analysis. The mobilized friction angle for each limiting equilibrium analyses is $\tan^{-1}\phi_{mob} = (\tan\phi)/1.3$. The mobilized friction angle for the apparent earth pressure diagram was computed by solving Equation 2.7.

$$\phi_{mob} = 2\left(45° - \tan^{-1}\left[\sqrt{1.3}\,\tan\left(45 - \frac{\phi}{2}\right)\right]\right) \qquad \ldots [2.7]$$

The factor of safety on shear strength for each analysis was expressed as $FS = \tan\phi/\tan\phi_{mob}$.

Lateral loads and the locations of the failure surfaces were similar for the limiting equilibrium methods. Computed load from the apparent earth pressure diagram was about 7 percent lower than the loads determined using limiting equilibrium methods. The difference in the loads is primarily a result of differences in the failure surfaces analyzed. Apparent earth pressure diagrams assume that the failure surface goes through the bottom corner of the excavation. Limiting equilibrium methods allowed failure surfaces to go below the bottom corner of the cut.

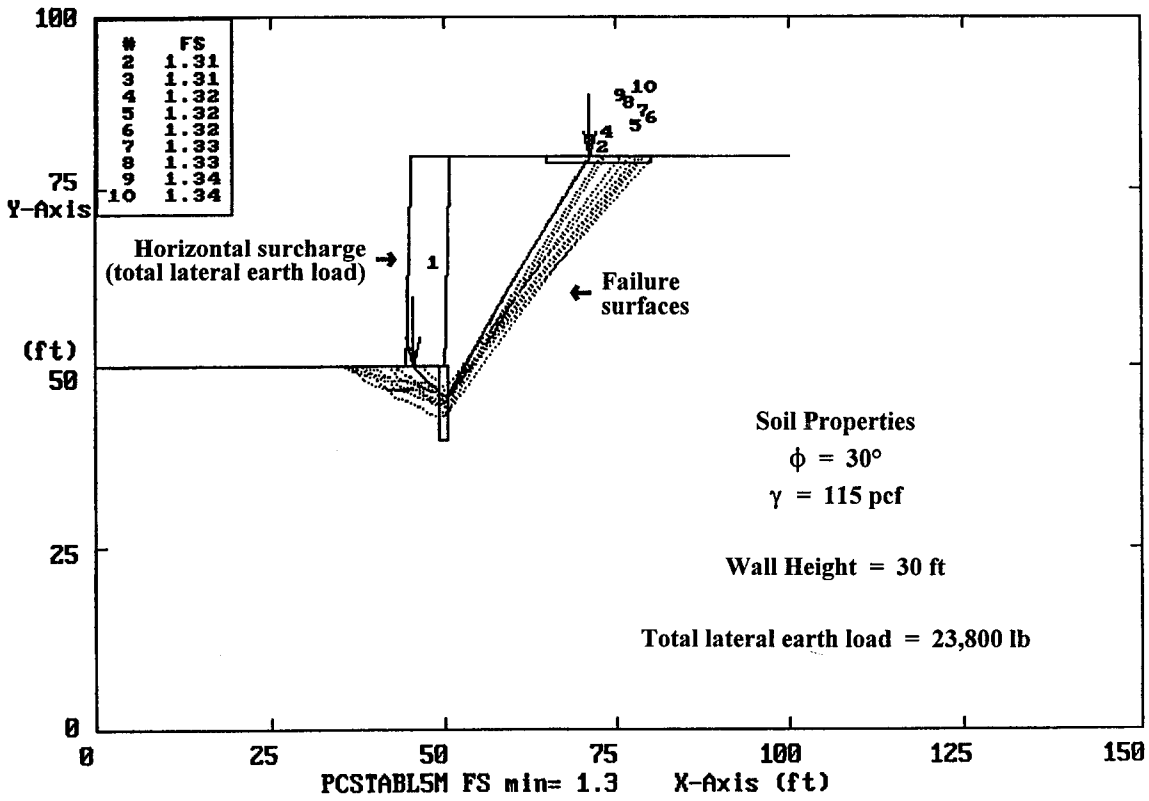


**FIGURE 12**
**Graphical Output from a STABL5M Analysis, *H* = 30 ft, ϕ = 30°, γ = 130 pcf**

**TABLE 4**
**Total Lateral Earth Loads Computed Using Limiting Equilibrium Methods and the Apparent Earth Pressure Diagram, *H* = 30 ft, ϕ = 30°, and γ = 115 pcf**

| CALCULATION METHOD | TOTAL LATERAL EARTH LOAD (lb) | MOBILIZED FICTION ANGLE (deg) | FS ON SOIL STRENGTH | DEPTH OF FAILURE SURFACE (ft) | ANGLE OF FAILURE SURFACE, α (deg) |
|---|---|---|---|---|---|
| Apparent Earth Pressure | 22402 | 23.29 | 1.34 | 0.00 | 56.7 |
| Force Equilibrium Method | 24028 | 23.95 | 1.30 | 3.00 | 56.0 |
| Computer | 23800 | 23.95 | 1.30 | 4.38 | 58.9 |

Table 4 shows that **the total lateral load for an anchored wall can be determined using apparent earth pressure diagrams or limiting equilibrium. When limiting equilibrium analyses are performed, use a factor of safety of 1.3 on the shear strength.**

**Before using a general purpose slope stability program for design, carefully check the program to ensure that it gives reasonable results. The total lateral load from the force equilibrium method or apparent earth pressure diagrams can be used to check the computer solution for several simple cases. The computer program and the force equilibrium method should give similar results. A factor of safety of 1.3 on the shear strength of the soil will give lateral earth loads similar to those estimated using Terzaghi and Peck's apparent earth pressure diagram for sand.**

When using a general purpose slope stability program to determine the total lateral earth load, do the following:

- **In sandy ground, select an analysis method that uses force equilibrium and planar failure surfaces (Janbu's Method (Janbu, et al., 1956)).**
- **For clayey soils, select a moment equilibrium method (Bishop's Method (Bishop, 1955)) and use circular failure surfaces for the analysis.**

**When the wall penetrates the failure surface, use a horizontal surcharge load in the stability analysis.** Here, the vertical component of the ground anchor load will be transmitted to the ground below the failure surface. **If the toe of the wall does not penetrate the failure surface, the surcharge load should be inclined at the same angle as the ground anchor.** When the wall does not penetrate the failure surface, the horizontal and vertical components of the ground anchor load are transmitted to the failure surface. Figure 13 illustrates the two different cases and shows how the ground anchor load should be modeled in the limiting equilibrium analyses.

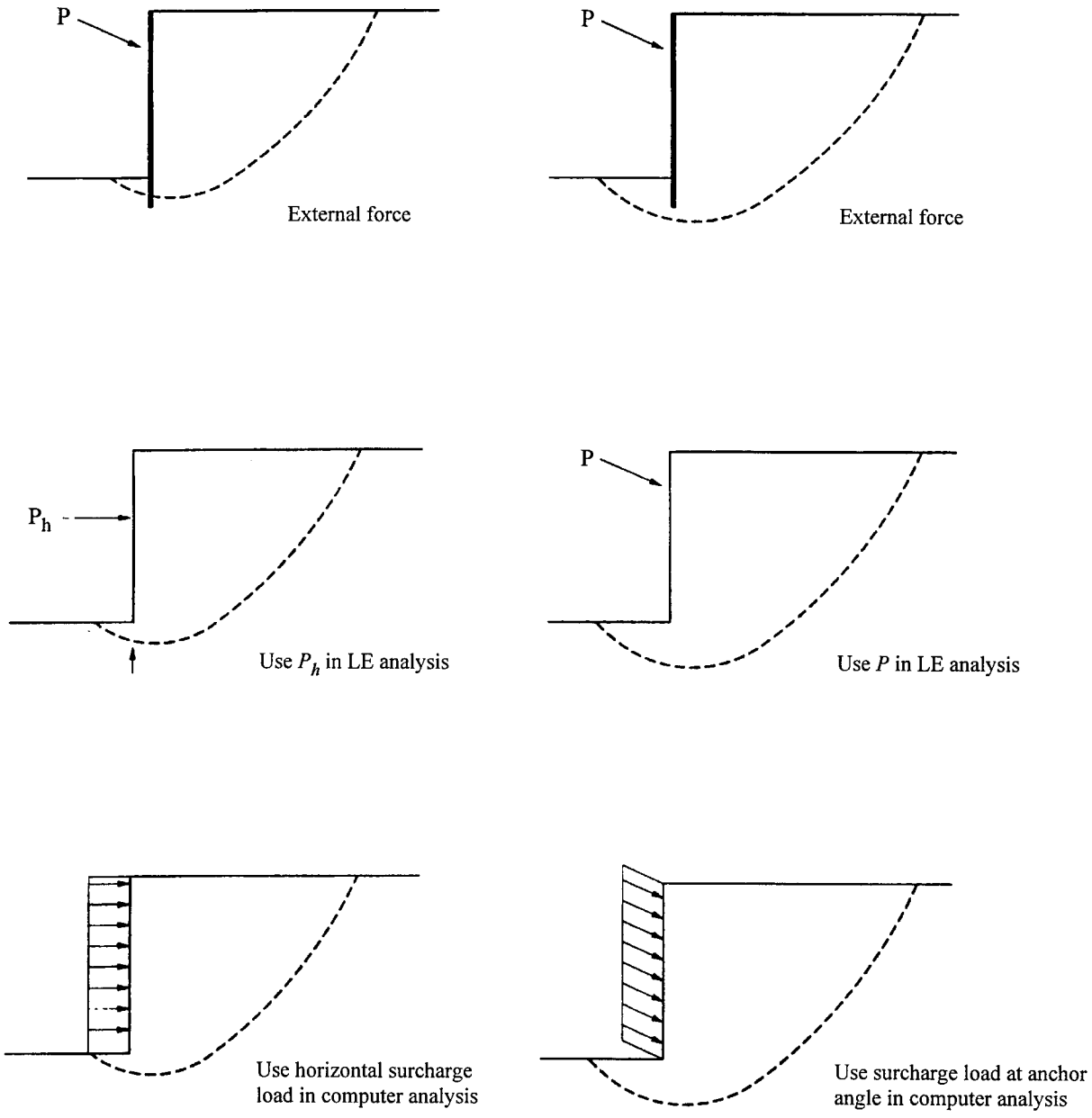


**FIGURE 13**
**Modeling of the Ground Anchor in Limiting Equilibrium Analysis**

### 2.1.5 Apparent Earth Pressure Diagram for Sand and Stiff Clay

Figures 14 and 15 show the modified trapezoidal apparent earth pressure diagrams for granular soils and stiff clay. The diagram in Figure 14 is for a wall supported by one row of anchors, and the diagram in Figure 15 is for a wall supported by multiple rows of anchors. The intensity of the pressure in these diagrams is calculated from the total lateral earth load. **Total lateral earth load for granular soils is the total load from Terzaghi and Peck's sand diagram ($0.65 K_a \gamma H^2$) or the load determined from a limiting equilibrium analysis. Total load for stiff clays is $20H^2$. Limiting equilibrium analyses cannot be used to calculate the total lateral load for a wall in stiff clay. The stiff clay apparent earth pressure diagram is used when the undrained shear strength of the fine-grained soil is greater than**

$$s_u \geq \frac{H}{4}(\gamma - 22.9) \qquad \ldots [2.8]$$

When the undrained strength is less than that given by Equation 2.8, then the soft to medium clay diagram is used (Sections 2.1.6 and 2.1.7). The total load for the granular soils and stiff fine-grained soils varies between a narrow range, $20H^2$ and $24H^2$. Additional discussion about the modified apparent earth pressure diagrams is contained in the *Summary Report of Research on Permanent Ground Anchor Walls*, "Volume II: Full-scale Wall Tests and a Soil-structure Interaction Model," (Weatherby, et al., 1998). **The modified trapezoidal diagram is the most appropriate diagram for the design of flexible, soldier beam walls supported by ground anchors** since:

- Measurements show that arching concentrates the earth pressures at the ground anchor locations.
- The earth pressures in a sand deposit must be zero at the ground surface.
- The trapezoidal diagram predicts support loads similar to those determined from the rectangular diagram.
- Trapezoidal apparent earth pressure diagrams model the earth pressures in stiff clays.
- Actual earth pressures increase from the ground surface to the ground anchor location.
- Bending moments predicted using the modified trapezoidal diagram fit measured results better than those predicted by other apparent earth pressure diagrams.
- Ground anchor loads determined from the non-symmetrical trapezoid diagram are similar to those determined using other apparent earth pressure diagrams.

Equations for determining the ground anchor loads and the soldier beam bending moments are presented in Figures 14 and 15. These equations use the tributary area method for determining ground anchor loads. The equation for the bending moment at the upper anchor sums moments about the anchor. Bending moment equations below the upper support are based on a moment factor and the maximum intensity of the earth pressure. Locations of the lower moments are not determined. These equations are easily incorporated into a spreadsheet.

**Long-term earth pressures for stiff-fissured clays may depend upon the drained shear strength of the soil** and could be higher than those determined using the stiff clay apparent earth pressure diagram. Compute earth pressures using drained sheared strengths and effective stresses. Design the wall to support the larger of the loads determined using undrained or drained shear strengths. See Section 2.1.8 for a discussion of lateral earth pressures based on drained shear strengths.

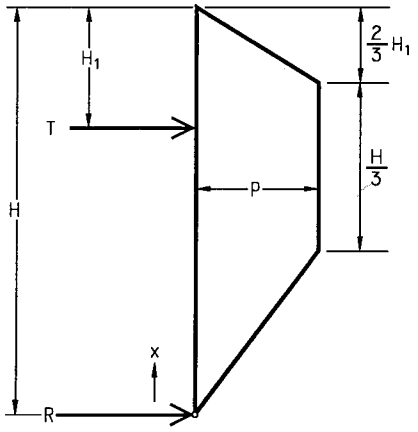


$$M_1 = \frac{13}{54} H_1^2 p$$

$$T_1 = \frac{(23H^2 - 10HH_1)}{54(H-H_1)} p$$

$$R = \frac{2}{3} Hp - T_1$$

Solve for point of zero shear

$$x = \frac{1}{9}\sqrt{26H^2 - 52HH_1}$$

$$MM_1 = Rx - \frac{px^3}{4(H-H_1)}$$

Earth Pressure "p" Determined from Total Load Required to Stabilize the Cut.

$$p = \frac{\text{Total Load}}{\frac{2}{3}H}$$

**FIGURE 14**
**Modified Trapezoidal Apparent Earth Pressure Diagram for Flexible Walls in Granular Soils and Stiff Clays and Supported by One Row of Anchors**

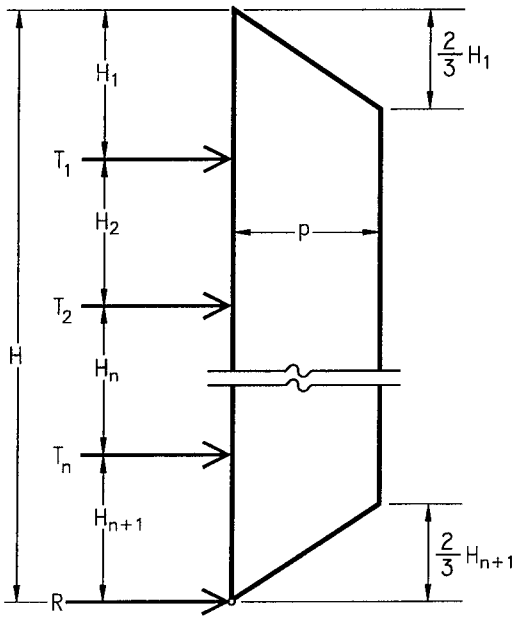


$$M_1 = \frac{13}{54} H_1^2 p$$

$$T_1 = (\frac{2}{3}H_1 + \frac{H_2}{2})p$$

$$MM_1 = \frac{1}{10} H_2^2 p$$

$$MM_2 = \frac{1}{10} H_3^2 p$$

$$MM_n = \frac{1}{10} H_{n+1}^2 p$$

$$MM_{n+1} = \frac{1}{10} H_{n+2}^2 p$$

$M_2$ = Larger of $MM_1$ or $MM_2$

$M_n$ = Larger of $MM_n$ or $MM_{n+1}$

$$T_2 = (\frac{H_2}{2} + \frac{H_n}{2})p$$

$$T_n = (\frac{H_n}{2} + \frac{23H_{n+1}}{48})p$$

$$R = (\frac{3}{16}H_{n+1})p$$

Earth Pressure "p" Determined from Total Load Required to Stabilize the Cut.

$$p = \frac{\text{Total Load}}{H - \frac{1}{3}H_1 - \frac{1}{3}H_{n+1}}$$

**FIGURE 15**
**Modified Trapezoidal Apparent Earth Pressure Diagram for Flexible Walls in Granular Soils and Stiff Clays and Supported by Multiple Rows of Anchors**

### 2.1.6 Apparent Earth Pressure Diagram for Soft to Medium Clay, No Deep-seated Failure

Temporary and permanent ground anchor walls in soft to medium clay must resist the short-term lateral earth pressures determined using undrained shear strengths and total unit weights. This section discusses the determination of these pressures when competent ground is at or near the bottom of the excavation. Section 2.1.7 discusses undrained analyses when weak soils lie below the bottom of the excavation. For permanent ground anchor walls, long-term earth pressures determined using drained shear strengths and effective stresses may be greater than pressures determined using undrained shear strengths. Section 2.1.8 discusses earth pressures developed using drained shear strengths.

**Lateral loads in a soft to medium clay are determined using Terzaghi and Peck's soft to medium clay apparent earth pressure diagram (Figure 4b) or limiting equilibrium analyses.** Earth pressures in soft to medium clay correspond to a state of limiting equilibrium. **A factor of safety on the shear strength of 1.3 should be used in analyses for permanent ground anchor walls.** Lower factors of safety have been used for temporary walls. When limiting equilibrium analyses are used, distribute the total load to the wall using the diagram shown in Figure 16.

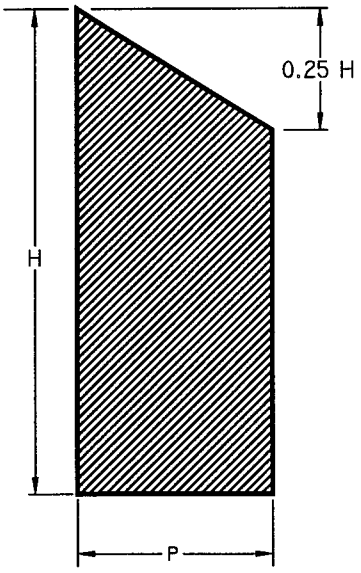


Intensity of Apparent Earth Pressure Diagram

$$p = \frac{\text{Total Lateral Earth Load}}{0.875H}$$

$$p = \left(1 - \frac{4s_u}{\gamma H}\right)\gamma H$$

**FIGURE 16**
**Apparent Earth Pressure Diagram for Soft Clay**

### 2.1.7 Apparent Earth Pressure Diagram for Soft to Medium Clay, Deep-seated Failure

**Permanent ground anchor walls are not recommended for sites where the bottom of the wall is underlain by deep deposits of weak soils.** Temporary earth retaining walls are built at these locations. Earth pressures computed from the soft to medium clay diagram (Figure 4b) under-estimate the total lateral earth load when weak soils extend below the bottom of the wall. Loads higher than those predicted develop when the soil below the wall yields. Limiting equilibrium analyses are recommended for determining the total lateral earth load on temporary earth retaining walls constructed in soft to medium clays and subject to deep-seated failures. Limiting equilibrium methods account for plastic yielding, basal heave, and the failure mechanism analyzed by Henkel (1971).

Use moment equilibrium methods with circular failure surfaces for limiting equilibrium analyses in soft to medium clay soils. Undrained shear strengths are used in the analysis. A factor of safety of 1.3 on the shear strength is commonly used. Since moment equilibrium methods are recommended, each ground anchor will have a different moment arm (Figure 17). Consequently, the stabilizing effect of each anchor will depend upon the magnitude of the anchor load and its moment arm. Two limiting equilibrium analyses are necessary to develop reasonable earth pressure diagrams for walls subject to a deep-seated failure. First, an analysis forcing the failure surfaces to go through the bottom corner of the wall is run. The second analysis is run allowing the failure surfaces to go below the bottom of the wall. In the second analysis, keep the surcharge load from the first analysis over the upper half of the wall, and apply a second surcharge load to the bottom half of the wall. Increase the lower surcharge load until the desired factor of safety is obtained. Construct an apparent earth pressure diagram from the two surcharge diagrams. Figure 18 illustrates how these two analyses are done. Bending moments and ground anchor loads are computed from the composite diagram.

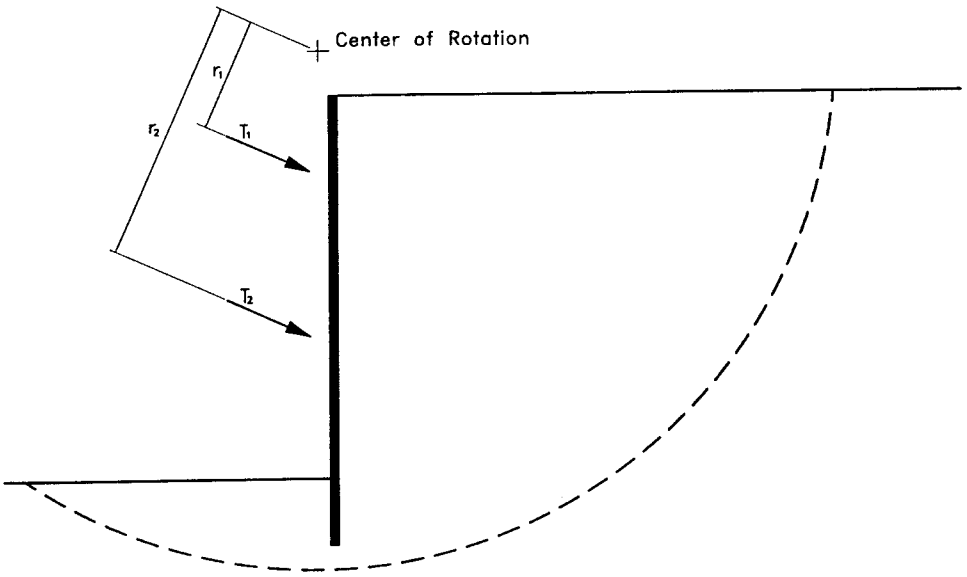


**FIGURE 17**
**Diagram Illustrating the Moment Arms for Ground Anchors in a Moment Equilibrium Stability Analysis**

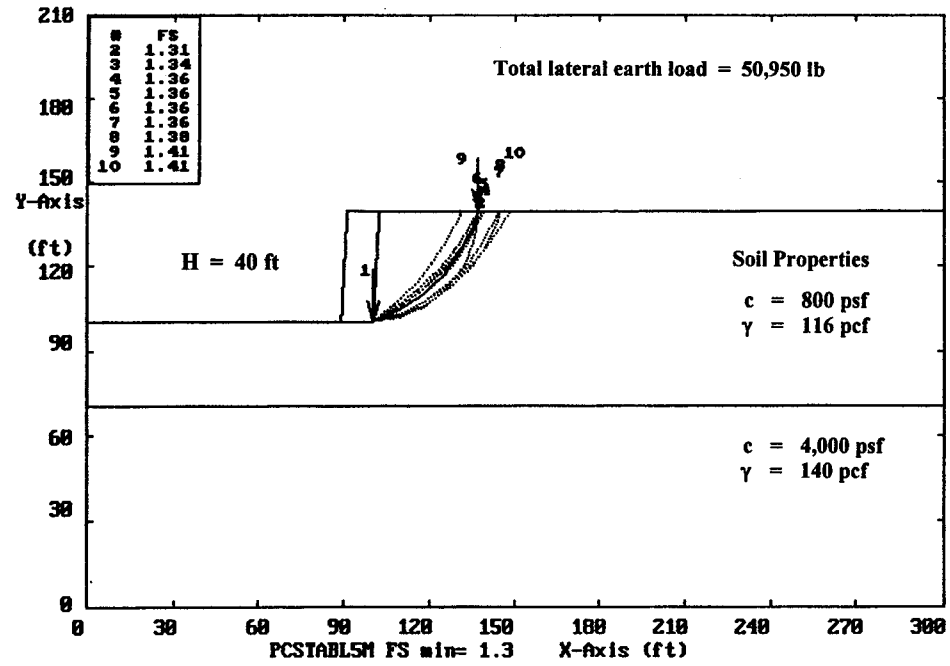


a) Load determined by analyzing failure surfaces through the bottom corner of the excavation

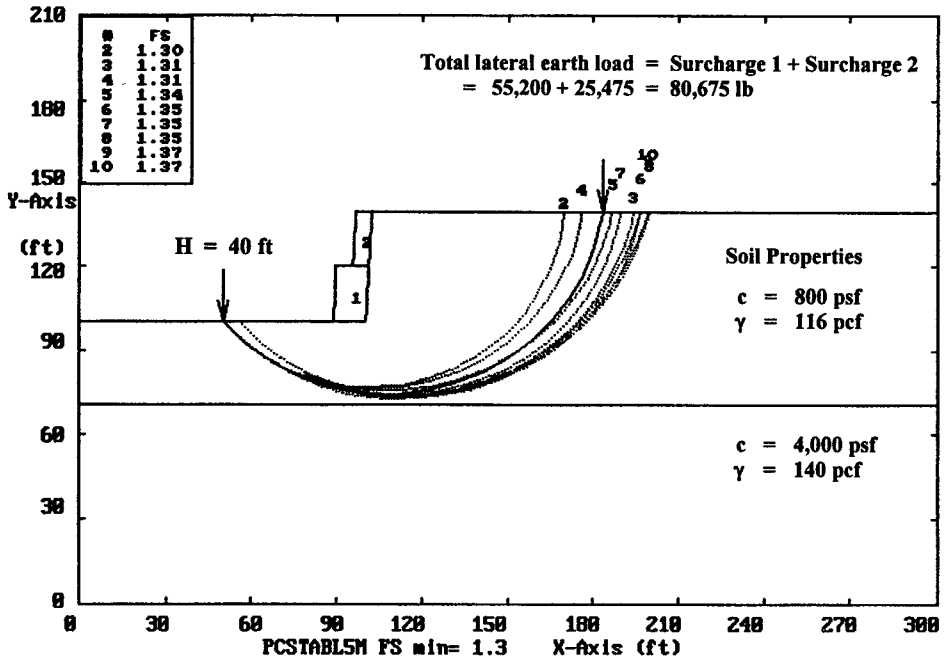


b) Load determined by analyzing deep-seated failure surfaces

**FIGURE 18**
**Example of Limiting Equilibrium Analyses for Determing Lateral Earth Pressures for Cuts in Soft to Medium Clay with Deep-seated Failures**

### 2.1.8 Apparent Earth Pressure Diagram for Clay, Drained Shear Strength

Apparent earth pressure diagrams for soft to medium clay relate the earth pressures to the undrained shear strength and the total unit weight of the soil. Diagrams for stiff fissured clays use a factor to determine the lateral earth pressures. Experience has shown that apparent earth pressure diagrams are valid for temporary earth support systems and they have been successfully used for the design of permanent ground anchor walls. However, anchored walls have not been in service long enough to determine whether fully drained conditions will develop in the soil behind the wall. **Since permanent ground anchor walls have a design life greater than 50 years, permanent ground anchor walls in cohesive soils are checked for earth pressures associated with drained shear strengths and effective stresses.** Design using drained strengths requires the selection of the correct shear strength parameters and the determination of the equilibrium porewater pressures within the ground behind the wall.

The drained shear strength of a given cohesive soil depends upon stress history (degree of overconsolidation), discontinuities (fissures, slickensides, joints, and shears), conditions during geological unloading, and associated swelling, weathering, and level of effective normal stress. **Drained shear strengths for a cohesive soil may be expressed as the normally consolidated (fully softened) shear strength, the intact strength of an overconsolidated clay, the destructured strength of an overconsolidated clay, or the residual strength** (Terzaghi, et al., 1996). Weatherby (1997) provides guidance for selecting the drained friction angle for fine-grained soils.

### 2.1.9 Checking Different Construction Stages

**It is unnecessary to check permanent ground anchor walls for intermediate construction stages if the wall is designed to resist apparent earth pressures, and the excavation does not extend too far below the anchor elevation before the anchor is locked-off.** The practice of checking bending moments and embedment depths for the "cantilever stage" excavation for the upper row of ground anchors developed because one-tier walls were designed for triangular earth pressures rather than apparent earth pressure diagrams. When triangular earth pressures are used, the ground anchor can be lower since the earth pressures are much less than the apparent earth pressures. Table 5 illustrates the differences in earth pressures, total load, and bending moments between the Rankine triangular pressure diagram and the modified trapezoidal apparent earth pressure diagram for a 25-ft-high wall with one row of anchors at 9 ft. The soil was assumed to have a Rankine active earth pressure coefficient of 0.307 and a total unit weight of 115 pcf. At the ground anchor elevation, the total lateral earth load from the apparent earth pressure diagram is 3.7 times greater than the total load from the Rankine triangular earth pressure diagram, and the bending moment from the apparent earth pressure diagram is 2.7 times greater than the bending moment from the triangular earth pressure diagram.

**TABLE 5**
**Comparison of Earth Pressures and Bending Moments at the Anchor Elevation for Triangular and Apparent Earth Pressure Diagrams**

| | RESULTS | |
|---|---|---|
| | Rankine Triangular Earth Pressure Diagram | Modified Trapezoidal Apparent Earth Pressures |
| Earth Pressures @ Ground Anchor Level (ksf) | 0.318 | 0.883 |
| Total Lateral Load Above Anchor Level (k/lf) | 1.431 | 5.298 |
| Bending Moment @ Ground Anchor Level (k-ft/lf) | 6.4 | 17.2 |

Field measurements also show that designing permanent ground anchor walls for intermediate construction stages is unnecessary. Figure 19 shows the measured bending moments for each stage of construction for a wall supported by one row of ground anchors, and a wall supported by two rows of ground anchors. The walls were 25 ft high and built in a medium-dense sand having a friction angle of 32° and a total unit weight of 115 pcf. Table 6 describes the construction stages associated with the moment curves in the figure. Figure 19 and the large-scale model tests described by Mueller, et al. (1998) show that **the maximum bending moments occurred when the excavation was completed, and the magnitudes of the bending moments at the final stage were predicted by the apparent earth pressure diagram.**

Stage construction analysis may be necessary for temporary walls in soft to medium clay or low-strength soils. When the ground in front of the wall is not adequate to support the toe laterally, the bending moments that develop before the next support is installed may be larger than the bending moments computed for the final construction condition.

**TABLE 6**
**Construction Stages for One- and Two-tier Wall in Figure 19**

| | ONE-TIER WALL | TWO-TIER WALL |
|---|---|---|
| Excavate to Upper Anchor | 10-ft excavation | 8-ft excavation |
| Install Upper Anchor | Stress T1 @ 9 ft | Stress T1 @ 6 ft |
| Excavate to Lower Anchor | | 17-ft excavation |
| Install Lower Anchor | | Stress T2 @ 16 ft |
| Final Excavation | 25-ft excavation | 25-ft excavation |

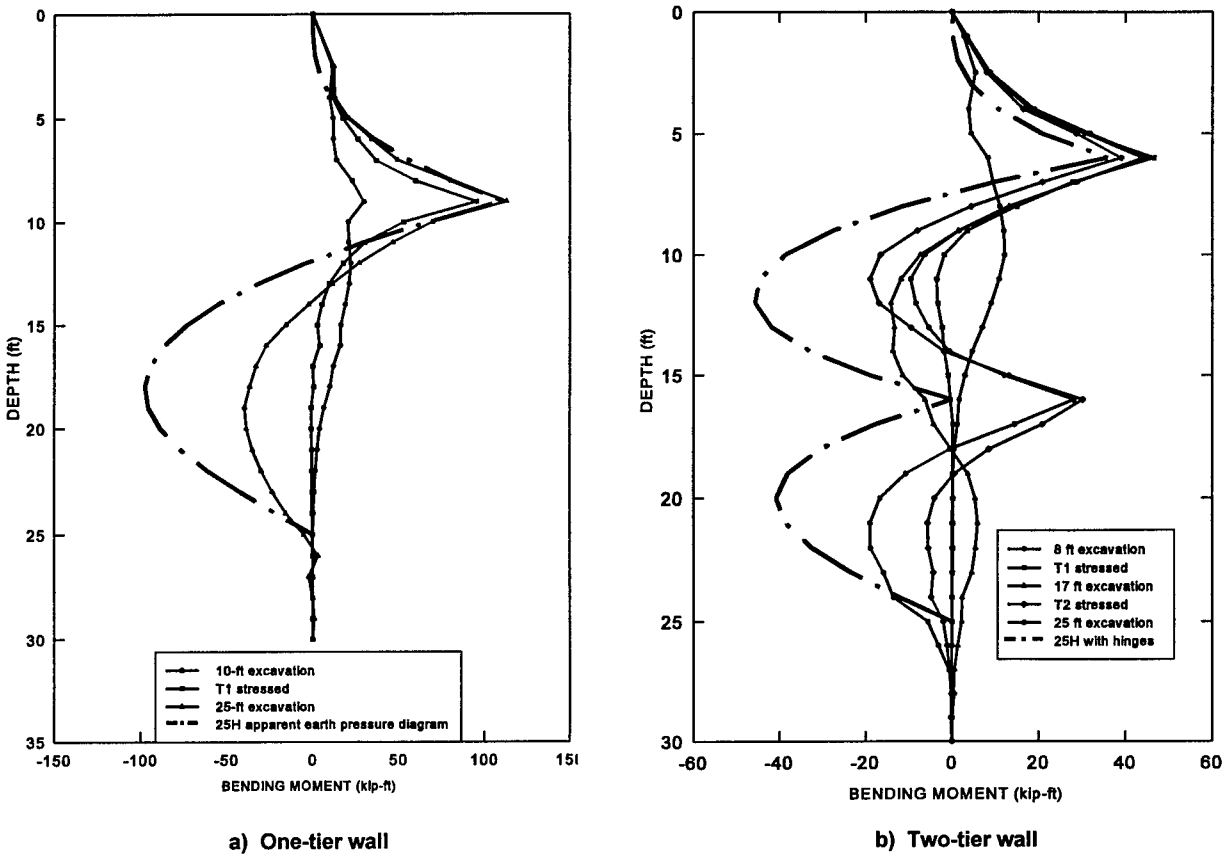


a) One-tier wall

b) Two-tier wall

**FIGURE 19**
**Measured Bending Moments for Each Stage of Construction for a 25-ft-high Wall**

### 2.1.10 Resisting the Upper Ground Anchor Test Load

**When the ground anchor loads are determined from apparent earth pressure diagrams, checking the passive capacity of the ground is unnecessary unless the ground has been disturbed.** When the ground behind the upper portion of the wall is disturbed or the ground anchor load is higher than the load determined from the apparent earth pressure diagram, the soldier beam may deflect excessively during testing of the upper ground anchor. High ground anchor loads result when the anchors are designed to support surcharge, barrier, or landslide loads. To resist the applied test load, the ground behind the soldier beam must develop sufficient passive resistance. If the ground anchor is designed to support loads greater then those given by the apparent earth pressure diagrams, then the passive capacity of the wall should be checked to determine if the ground can resist the upper ground anchor test load.

Weatherby, et al. (1998) developed an earth pressure calculation to check the passive capacity of the soldier beam to resist the test load applied to the upper ground anchor. The assumption

behind the calculation is that the lateral resistance will be developed over a depth of 1.5 times the distance to the upper ground anchor. Equation 2.9 gives the passive resistance.

$$1.125 K_p \gamma h_1^2 s \quad \ldots [2.9]$$

In Equation 2.9, $K_p$ is determined using Figure 10, and $h_1$ is the depth to the upper ground anchor.

## 2.2 AXIAL AND LATERAL LOAD BEHAVIOR OF THE TOE

The embedded portion of a ground anchor wall, the toe, must resist vertical and lateral loads. Vertical loads are caused by the ground anchors and other applied loads, and lateral load results from the earth pressures. Figure 20 illustrates skin friction and end bearing mobilized to resist the axial loads in the wall, and lateral resistance mobilized to resist the toe reaction from the apparent earth pressure diagram.

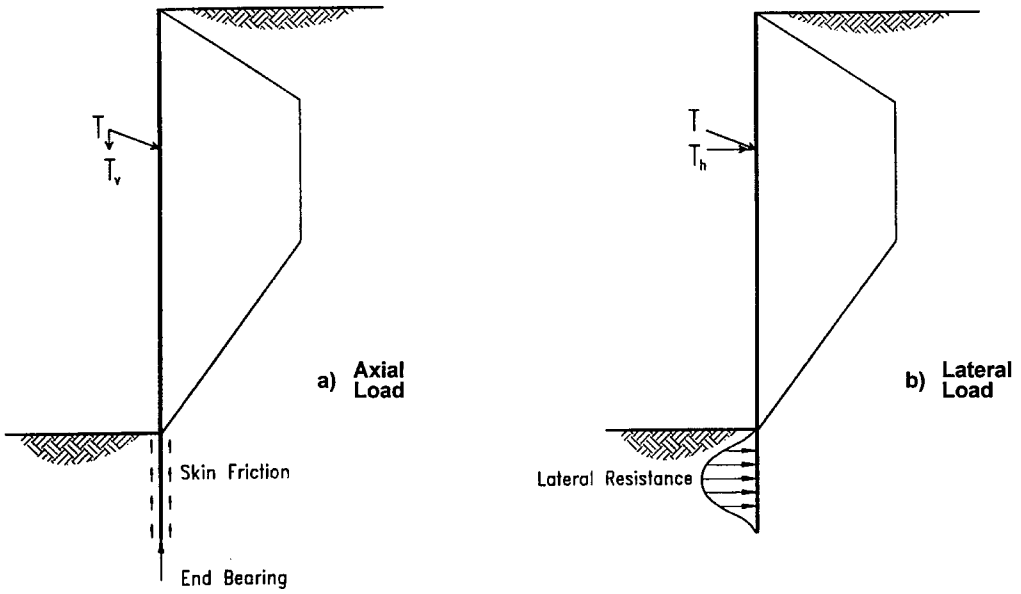


**FIGURE 20**
**Diagram Illustrating the Axial and Lateral Loads on an Anchored Wall Toe**

### 2.2.1 Axial Load

**The magnitude of the axial load depends upon: the vertical components of the ground anchor loads, the strength of the supported ground, vertical and lateral movements of the wall, the relative movements of the ground with respect to the wall, and the axial load-carrying capacity of the toe.** Axial load transferred to a soldier beam toe can be less than or

more than the vertical components of the anchor loads (Figure 21). Axial loads in the wall are greater than the vertical components of the ground anchor loads if the ground behind the wall settles relative to the wall. When the wall settles relative to the ground, the axial load in the wall is less than the vertical component of the ground anchor.

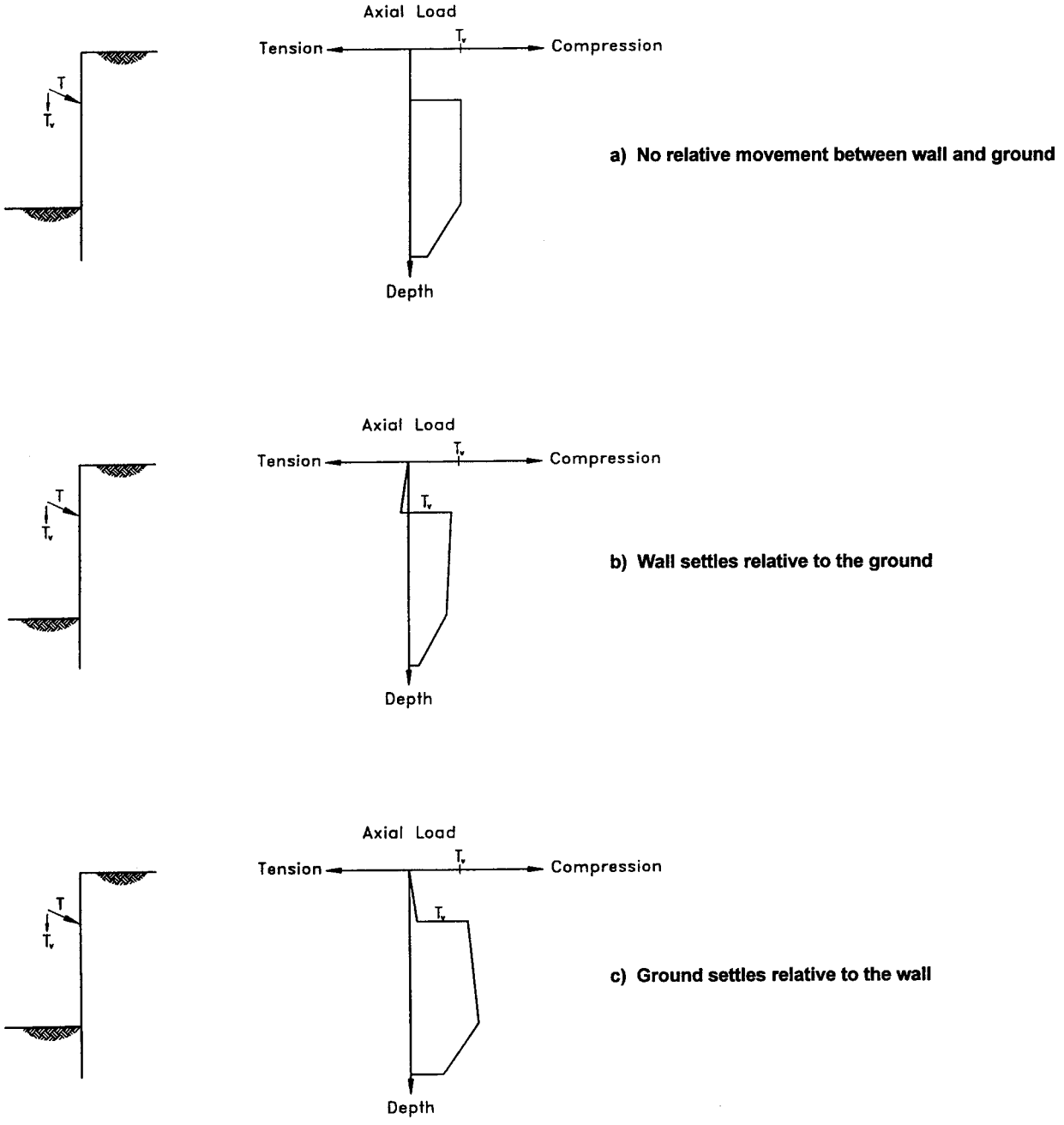


**FIGURE 21**
**Idealized Axial Load Distributions for Soldier Beam Walls**

**Determine the axial load to be resisted by the toe of an anchored wall using the guidelines in Table 7. Axial load transferred to the toe includes the vertical components of the ground anchor loads plus applied loads minus the load transferred to the ground above the bottom of the excavation.** Load is transferred to the ground above the bottom of the excavation when the shear strength of the ground is high. The recommendations in Table 7 do not include downdrag loads. If downdrag loads develop, they will be transferred to the ground after small wall settlements.

**TABLE 7**
**Guidelines for Estimating the Axial Load Applied to the Toe**

| SANDS | | CLAYS | |
|---|---|---|---|
| **Medium Dense** | **Dense to Very Dense** | **Soft to Medium** | **Stiff** |
| $10 \le SPT \le 30$ | $SPT > 30$ | $s_u \le \gamma H/4 - 5.714H$ | $s_u > \gamma H/4 - 5.714H$ |
| I | II | I | III |

| | |
|---|---|
| I | Design toe to resist vertical components of the ground anchor loads plus applied axial loads |
| II | Design toe to resist vertical components of the ground anchor loads plus applied axial loads minus the horizontal components of the ground anchor loads times tanδ (δ between $\phi/4$ and $\phi/2$) |
| III | Design toe to resist vertical components of the ground anchor loads plus applied axial loads minus $A_s \cdot 0.25 s_u$ ($A_s$ = surface area of steel in contact with the ground and $s_u$ = undrained shear strength) |

The ultimate axial load-carrying capacity of a soldier beam is determined using relationships for either driven piles or drilled shafts. **Use the average effective overburden pressure when determining the skin friction resistance.** The effective overburden pressure on one side of the soldier beam depends upon a depth of embedment from the ground surface to the midpoint of the toe. On the other side of the beam, the effective overburden pressure depends upon the embedment depth from the bottom of the excavation to the midpoint of the toe. **The toe embedment is used when determining the end bearing resistance for driven soldier beams. Use the block perimeter area for skin friction and end bearing calculations for driven H-beam sections.**

Drilled-in soldier beams may be backfilled with lean-mix fill or structural concrete. When structural concrete is used, the axial capacity is determined using drilled shaft relationships. **When lean mix fill is used, determine the axial capacity for a beam punching through the lean mix and the capacity for a drilled shaft. The smallest capacity is used in the design.**

**Axial load transferred to the toe will be zero or very small if the ground anchors are installed at an angle equal to half the soil friction angle.**

**Use a factor of safety of 2 for the axial load design of permanent ground anchor wall toes.** A factor of safety of 2 is adequate since the wall will remain serviceable if the axial capacity of the toe is exceeded. When the toe of an anchored wall is overloaded, the wall will settle slightly and transfer load to the ground until equilibrium is reached.

### 2.2.2 Lateral Load

**Anchored wall toes must carry the lateral loads resulting from the earth pressures with an adequate factor of safety. Apparent earth pressure calculation methods determine a concentrated lateral load, called the toe reaction, at a hinge at the bottom corner of the excavation. Passive resistance mobilized in front of the toe must be adequate to resist the toe reaction with a factor of safety of 1.5. Permanent ground anchor walls should not be constructed in ground that does not have adequate lateral support for the toe of the wall. If a temporary excavation support system is used in ground with insufficient strength to resist the subgrade reaction, then the wall must be designed to cantilever around the lowest support.**

Relationships developed by Wang and Reese (1986) describe the ultimate lateral toe resistance of a soldier beam wall (Weatherby, et al., 1998). They considered three modes of failure and developed equations for the passive resistance at any depth for sands and clays. To incorporate their equations in the design of anchored walls, the ultimate resistances for each failure mode are determined, and the smallest resistance is used to describe the passive resistance of the toe at any depth. The different failure mechanisms in sand are presented to illustrate the concept. Figures showing similar failure mechanisms for clay are presented in Section 2.2.2.2. One mode of failure assumes that the passive resistance results from a wedge failure in front of an individual soldier beam (Figure 22). When the soldier beams become too close or too deep, the individual wedges will overlap and the lateral resistance for an individual beam will be reduced (Figure 23). At some depth, the soil in front of the beam will be confined and the lateral resistance will not depend upon a wedge failure, but it will be limited by flow of the soil around the beam. Flow resistance will control when the soil plastically flows (Figure 24) between the soldier beams rather than a wedge failure up to the surface. Lateral resistance can be limited by a fourth failure mode not considered by Wang and Reese. At no point can the passive resistance be greater than that computed for a two-dimensional failure surface (Figure 25).

Equations for each failure mode are presented here. Those interested in studying their derivation are directed to the work by Wang and Reese (1986) and the *COM624 Manual* (Wang and Reese, 1992).

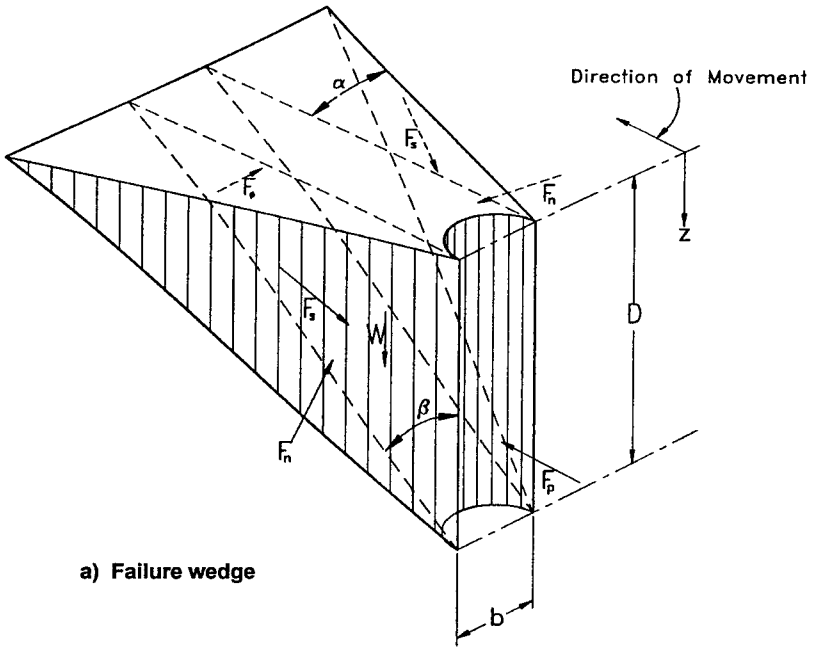


a) Failure wedge

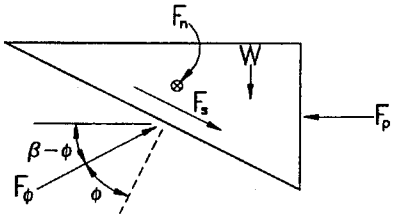


b) Forces on the wedge

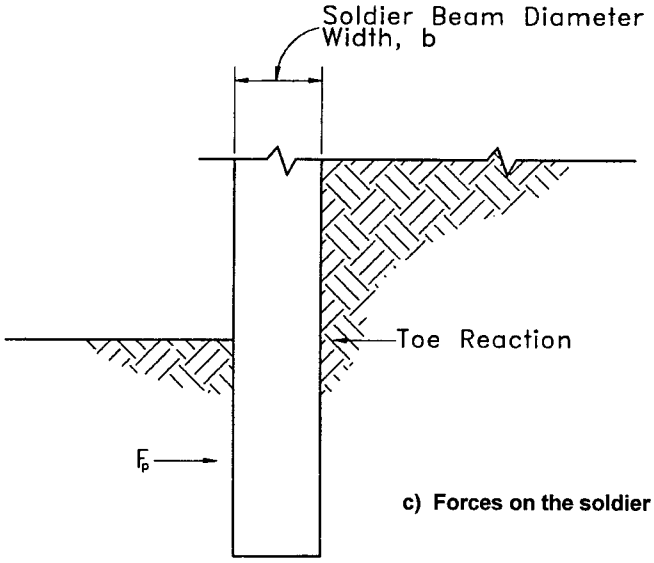


c) Forces on the soldier beam

**FIGURE 22**
**Passive Wedge Failure for a Soldier Beam in Sand (after Reese, et al., 1974)**

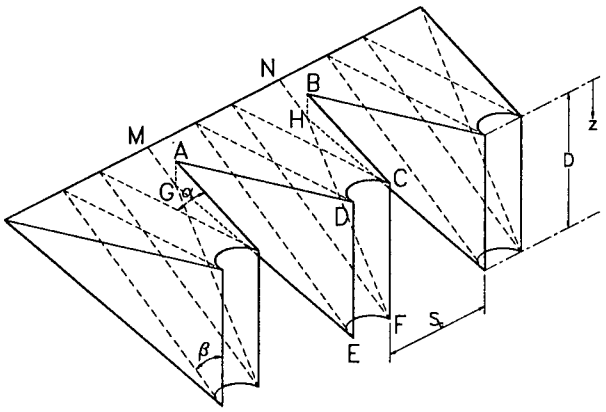


a) General view

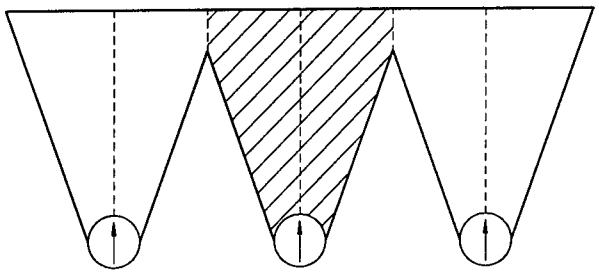

b) Plan view

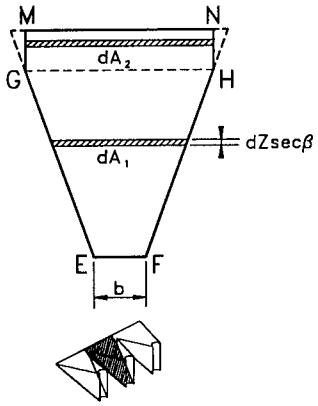


c) Bottom of a wedge

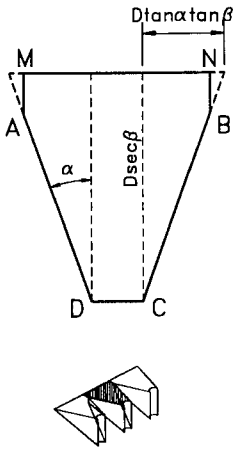


d) Top of a wedge

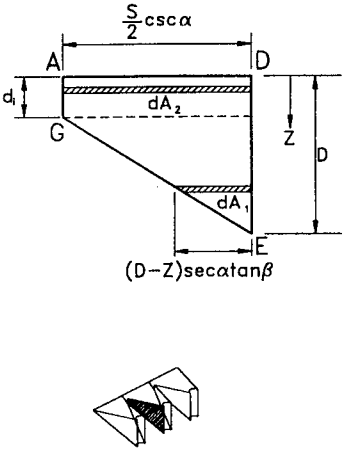


e) Side of a wedge

**FIGURE 23**
**Intersecting Failure Wedges for Soldier Beams in Sand**
**(after Wang and Reese, 1986)**

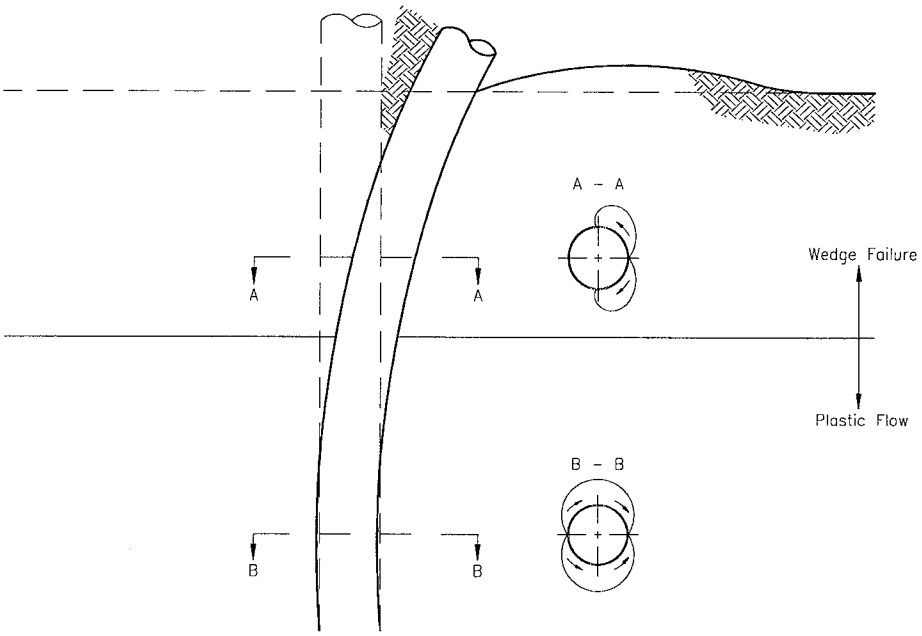


**FIGURE 24**
**Plastic Soil Flow Around a Soldier Beam Toe**
**(after Wang and Reese, 1986)**

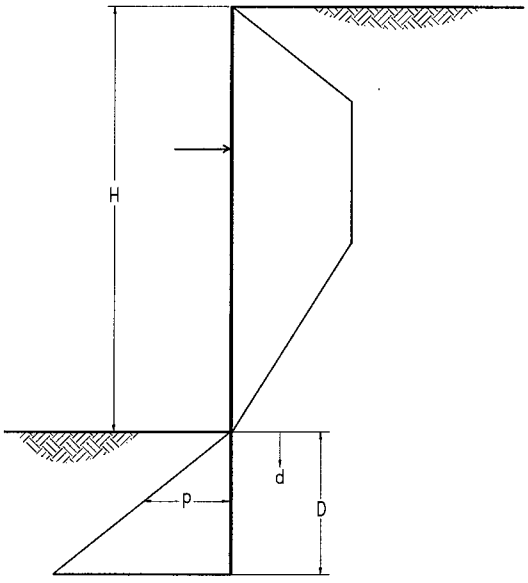


$p = (K_p \sigma'_v d)(s_c + b)$

$K_p$ = Passive earth pressure coefficient

$\sigma'v$ = Effective vertical stress

d = Distance

D = Toe penetration

$s_c$ = Clear spacing between soldier beams

b = Soldier beam width or diameter

**FIGURE 25**
**Passive Resistance for a Continuous Wall in Sand**

### 2.2.2.1 Passive Resistances in Sands

Figure 22 shows the wedge failure for a single soldier beam in sand. The passive force, $F_p$, is given by Equation 2.10 when the groundwater is below the tip of the soldier beam.

$$F_p = \gamma_{ave} D^2 \left[ \frac{K_o D \tan\phi \sin\beta}{3 \tan(\beta-\phi)\cos\alpha} + \frac{\tan\beta}{\tan(\beta-\phi)} \left( \frac{b}{2} + \frac{D}{3} \tan\beta \tan\alpha \right) + \frac{K_o D \tan\beta}{3} (\tan\phi - \sin\beta - \tan\alpha) \right] \quad \ldots [2.10]$$

where:

$\gamma_{ave}$ = average total unit weight
$K_o$ = at-rest earth pressure coefficient
$K_a$ = active earth pressure coefficient
$\beta = 45 + \phi/2$
$\alpha$ = $\phi$ for dense sands, $\phi/3 - \phi/2$ for loose sands

Equation 2.10 is differentiated to give the ultimate soil resistance at depth, $d$ (Equation 2.11).

$$p = \gamma d \left[ \frac{K_o d \tan\phi \sin\beta}{\tan(\beta-\phi)\cos\alpha} + \frac{\tan\beta}{\tan(\beta-\phi)} (b + d \tan\beta \tan\alpha) + K_o d \tan\beta (\tan\phi \sin\beta - \tan\alpha) \right] \quad \ldots [2.11]$$

Figure 23 shows the individual failure wedges intersecting as the soldier beams get closer or as the toe depth increases. Equation 2.12 gives the depth of the intersection of adjacent wedges.

$$d_i = D - \frac{s_c}{2 \tan\alpha \tan\beta} \quad \ldots [2.12]$$

where:

$D$ = toe depth
$s_c$ = clear spacing between soldier beams

When $d_i$ is positive, the failure wedges intersect. If $d_i$ is negative, the failure wedges do not intersect. At depths greater than $d_i$, the passive resistances are not affected by adjacent soldier beams, and they are computed using Equation 2.11. Above the point of intersection, the passive resistances are reduced to account for the intersection of the failure wedges. To account for the intersection of the wedges, the passive resistances determined from Equation 2.11 are reduced by the resistances determined for a wedge with a height, $d_i$, and a soldier beam with a width of zero. The resistances down to the depth, $d_i$, are given by Equation 2.13.

$$p = \gamma d \left[ \frac{K_o d \tan\phi \sin\beta}{\tan(\beta-\phi)} \left( \frac{1}{\cos\alpha} - 1 \right) + \frac{d \tan\beta \tan\alpha}{\tan(\beta-\phi)} - K_o d \frac{\sin^2\beta}{\cos\beta} \tan\phi (\tan\alpha + 1) \right] \quad \ldots [2.13]$$

where:

$d \le d_i$

At depth, the ultimate lateral resistance will be limited to the resistance that can develop before the soil flows between the soldier beams (Figure 24). Equation 2.14 gives the ultimate lateral flow resistance.

$$p = K_a b \gamma d \tan^8 \beta + K_o \gamma d \tan\phi \tan^4 \beta \quad \ldots [2.14]$$

Figure 25 shows the two-dimensional failure wedge. Lateral resistances cannot exceed the value given by Equation 2.15.

$$p = K_p \gamma d (s_c + b) \quad \ldots [2.15]$$

where:

$s_c$ = clear spacing between soldier beams

$b$ = soldier beam width or shaft diameter

Equations 2.11 to 2.15 give the passive resistance at a location. Rankine active pressures must be applied to the other side of the wall when computing the capacity of the toe (Figure 26).

**For drilled-in soldier beams backfilled with lean-mix fill use the steel soldier beam width when computing the passive resistance of the toe. If structural concrete is placed in the toe, the diameter of the drilled shaft can be used in the calculations.**

Equations 2.11 to 2.15 can be implemented in a spreadsheet to determine the lateral resistance. When the groundwater level is near the bottom of the excavation, use buoyant unit weights in Equations 2.11 to 2.15. *Design Manual for Permanent Ground Anchor Walls* (Weatherby, 1997) describes how the lateral toe resistance is determined when the groundwater level is a reasonable distance below the bottom of the excavation.

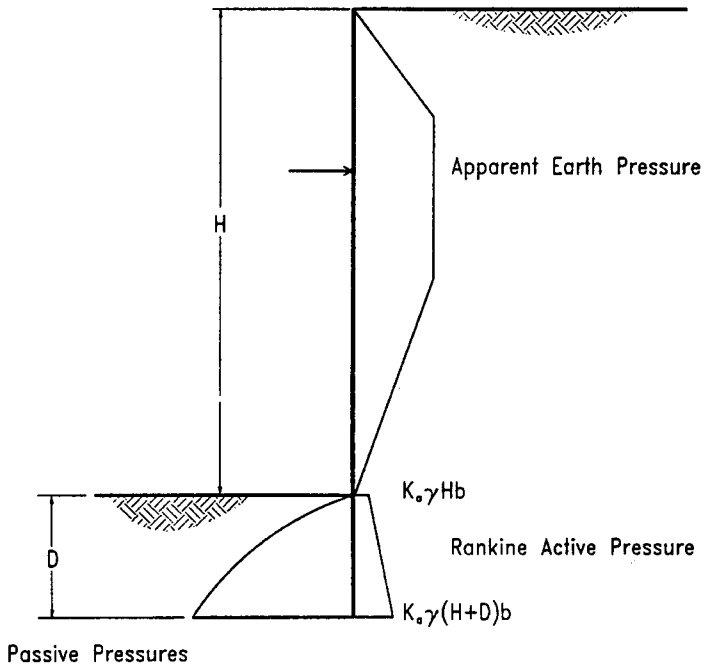


**FIGURE 26**
**Diagram Illustrating the Active and Passive Pressures on a Soldier Beam Toe in Sand**

### 2.2.2.2 Passive Resistances in Clays

Figure 27 shows the failure wedge for a single soldier beam in clay. Reese (1958) developed the expression for the passive resistance, $F_p$,

$$F_p = s_u D\,[\tan\theta + (1+K)\cot\theta] + \frac{1}{2}\gamma_{ave}\, b\, D^2 + s_u D^2 \sec\theta \qquad \ldots [2.16]$$

where:

$s_u$ = average undrained shear strength

$K$ = a reduction factor to apply to $s_u$ to give the adhesion between the soldier beam & the clay

$\gamma_{ave}$ = average total unit weight of soil (the other terms are defined in the figure)

Assuming $\theta = 45°$ and the shaft friction, $K = 0$, Equation 2.16 is differentiated to give the ultimate soil resistance at depth, $d$ (Equation 2.17).

$$p = 2 s_u b + \gamma b d + 2.83 s_u d \qquad \ldots [2.17]$$

Soldier beams in clay may be close enough that the wedge of soil between the beams is not adequate to develop the full shear resistance (forces $F_3$ and $F_4$ in Figure 27) on the sides of the wedge directly in front of the soldier beam. Figure 28 shows the passive wedges in front of each soldier beam and the wedge of soil between the beams (block FDBGHI). If the space between the beams is large, block FDBGHI will be adequate to resist the side shear forces $F_3$ and $F_4$ from the wedges in front of the beams. If block FDBGHI is small, then the entire ground in front of the wall will move together and the individual wedges in front of each beam will not develop. Wang and Reese (1986) developed expressions to describe the passive resistance of a row of drilled shafts (soldier beams) in clay. Equation 2.18 gives the critical spacing where the behavior changes from single beam behavior to group behavior.

$$S_{cr} = \frac{2.828\, s_u D}{\gamma_{ave} D + 6 s_u} \qquad \ldots [2.18]$$

Wang and Reese's passive resistance for a soldier beam considering group behavior is given by Equation 2.19.

$$p = 2 s_u (b + s_c) + \gamma_{ave} (b + s_u) d + s_u s_c \qquad \ldots [2.19]$$

If the spacing between soldier beams becomes zero and the soldier beam width is taken as unity, Equation 2.19 becomes Equation 2.20, the passive earth pressure equation for a continuous wall.

$$p = 2 s_u + \gamma_{ave} d \qquad \ldots [2.20]$$

When the toe of the soldier beam extends deep enough below the ground, the soil may flow around the beam as it moves through the soil. The failure is similar to that shown in Figure 24. Wang and Reese (1986) expressed the passive flow resistance in a clay to be approximately (Equation 2.21):

$$p = 11 s_u b \qquad \ldots [2.21]$$

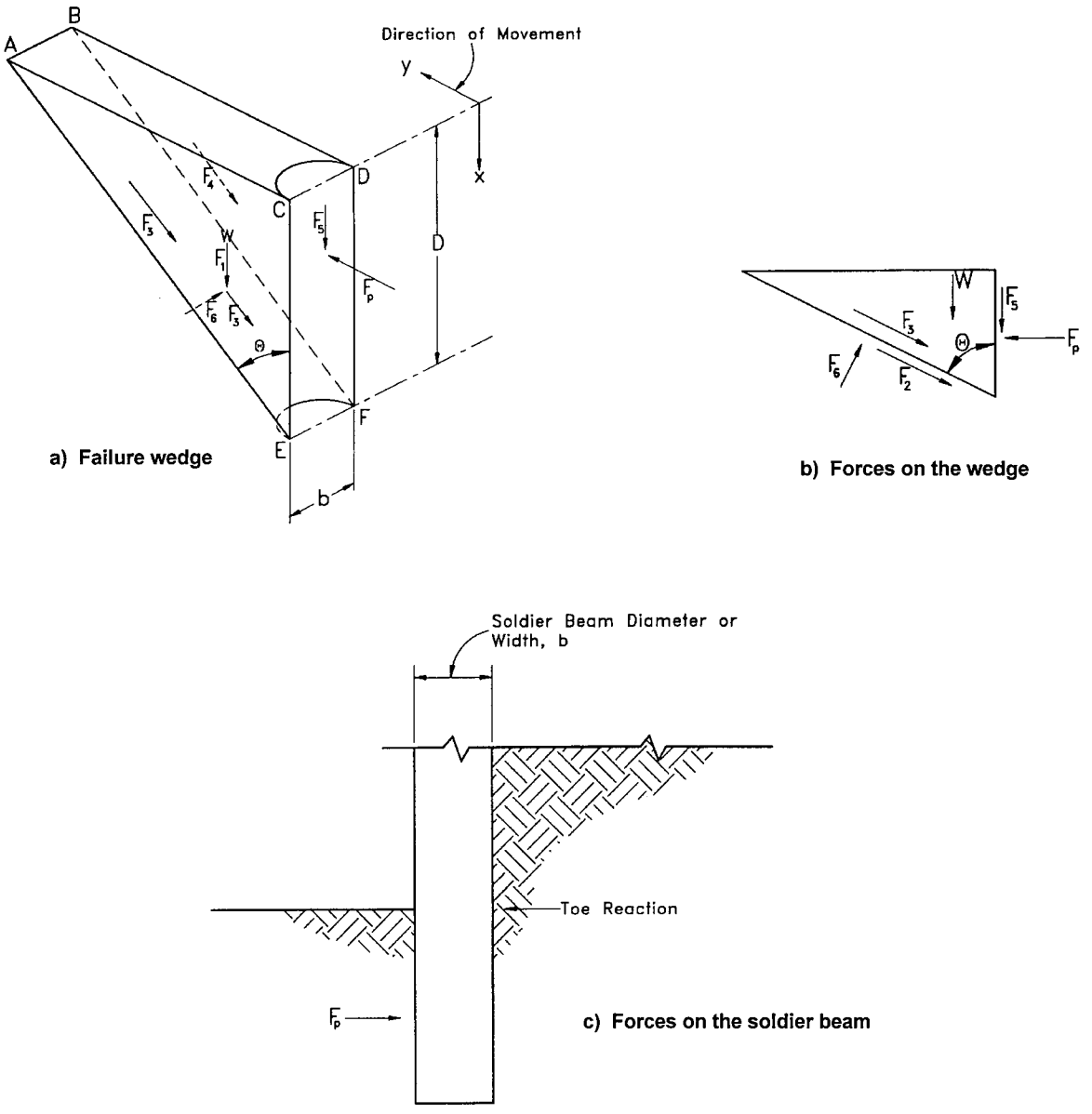


**FIGURE 27**
**Passive Wedge Failure for a Soldier Beam in Clay (after Reese, 1958)**

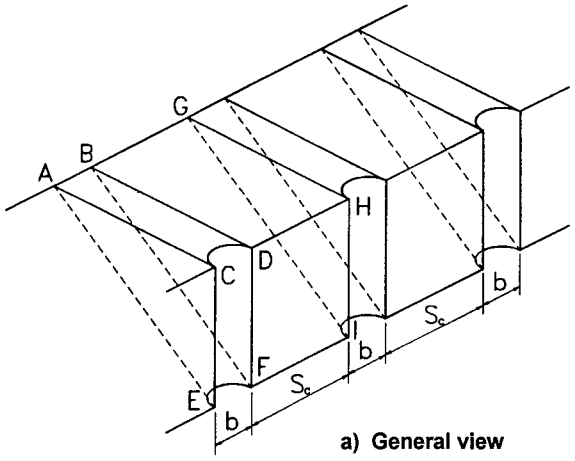


a) General view

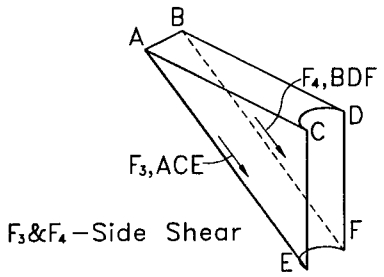


b) Wedge in front of soldier beam

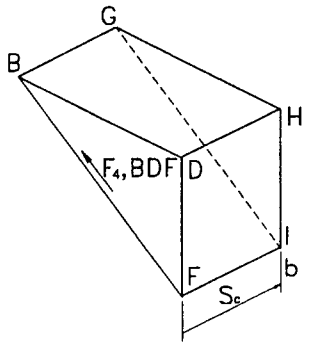


c) Block of soil between beams

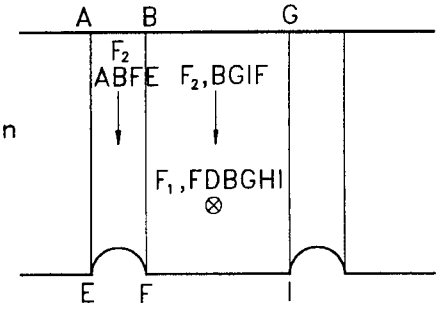


$F_2$ – Shear Resistance on Bottom of Wedges

$F_1$ – Weight Block

d) Plan view

**FIGURE 28**
**Failure Wedges for Adjacent Soldier Beams in Clay (after Wang and Reese, 1986)**

Figure 29 shows the two-dimensional failure wedge that limits the passive resistance that can develop. For a wall in clay the lateral resistance at any depth, $d$, cannot exceed the value given by Equation 2.22.

$$p = (2s_u + \gamma_{ave} d)\ (s_c + b) \qquad \ldots [2.22]$$

In stiff clays the active pressure may be negative behind the wall. Considering negative pressures during design is not reasonable since the soldier beam will move away from the soil. A continuous wall normally will be used when the active pressures are positive. Positive active pressures below the bottom of the excavation are given by Equation 2.23.

$$p_{active} = \gamma_{ave} (H + d) - 2s_u \qquad \ldots [2.23]$$

where:

$H$ = height of wall

Steel soldier beam width is used in Equations 2.16 to 2.23 for drilled shafts backfilled with lean mix, and the drilled shaft diameter is used when structural concrete is used to backfill the shaft.

Equations 2.16 to 2.23 can be implemented in a spreadsheet for determining the lateral toe resistance for a soldier beam in clay.

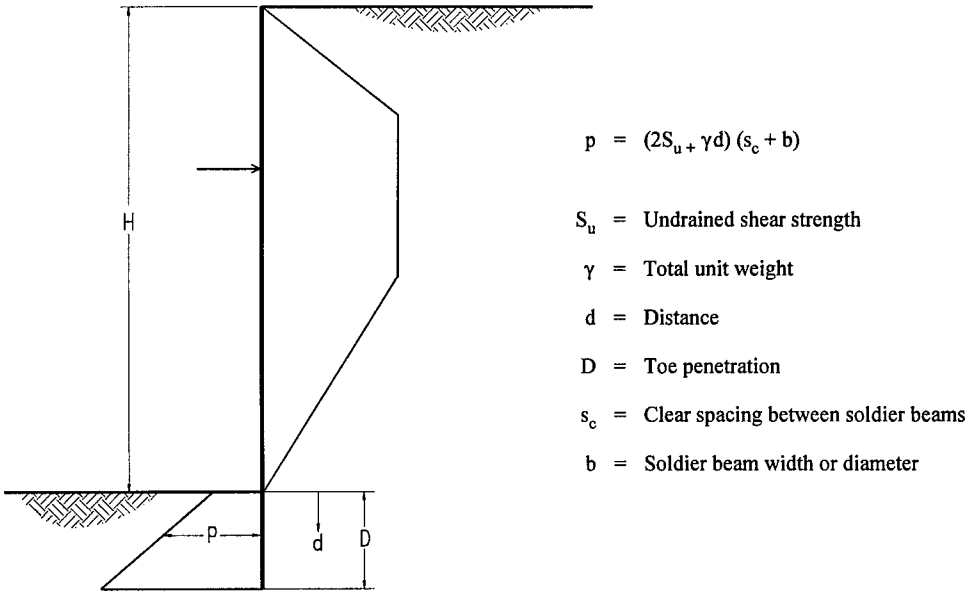


**FIGURE 29**
**Passive Resistance for a Continuous Wall in Clay**

## 2.3 DETERMINING ANCHOR LOAD(S), BENDING MOMENTS, AND TOE DEPTH

**Determine the ground anchor loads, soldier beam bending moments, and the toe embedment by:**

1. **Determining the total lateral load to be supported by the wall.**
   a. **Sand - 0.65 $K_a \gamma H^2$ (Section 2.1.5) or limiting equilibrium (Section 2.1.4).**
   b. **Stiff clay - 20 $H^2$ (Section 2.1.5).**
   c. **Soft clay no deep-seated failure - 0.875 $(1 - (4s_u)/(\gamma H))\gamma H^2$ (Section 2.1.6) or limiting equilibrium (Section 2.1.4).**
   d. **Surcharge loads**

2. **Selecting an appropriate apparent earth pressure diagram to distribute the load to the wall (Sections 2.1.5 and 2.1.6).**

3. **Selecting either the tributary area method or the simple beam method to determine anchor loads and bending moments (Section 2.1.2—Figure 5).**

4. **Solving equations for determining the anchor loads, bending moments, and reaction at subgrade. Assume the soldier beam is hinged at subgrade (Section 2.1.2—Figure 5, Section 2.1.5—Figures 14 and 15).**

5. **Selecting soldier beam spacing and size.**

6. **Determining the toe embedment required to develop a lateral toe resistance with an $FS \geq 1.5$ (Section 2.2.2).**

7. **Selecting ground anchor inclinations and computing anchor design loads.**

8. **Determining vertical components of ground anchor load and the load transferred to the toe (Section 2.2.1).**

9. **Determining the toe embedment required to develop the axial load with an $FS \geq 2.0$ (Section 2.2.1).**

## 2.4 SOIL-STRUCTURE INTERACTION ANALYSIS USING APPARENT EARTH PRESSURE DIAGRAMS AND *R-y* CURVES TO MODEL THE LATERAL TOE RESISTANCE

A computer program, *TB Wall — Anchored Wall Design and Analysis Program for Personal Computers* (Urzua and Weatherby, 1998), was developed to allow a soldier beam or sheet pile wall to be modeled as a continuous beam in a soil-structure interaction analysis. Earth pres-

sures above the bottom of the excavation in the analysis are given by an apparent earth pressure diagram selected by the user. Figure 30 conceptually illustrates how the earth pressures, toe resistance, and ground anchors are modeled. Below the bottom of the wall, the passive toe resistance is modeled by a series $R$-$y$ curves (soil springs). $R$-$y$ curves relate the resistance of the wall at a point to the deflection of the wall. Active $R_a$-$y$ curves are on the back of the wall, and passive $R_p$-$y$ curves were on the front of the wall. The maximum resistance is related to the resistance computed using the Wang and Reese relationships (Section 2.2.2). The minimum resistance is related to the active earth pressure. In *TB Wall*, the maximum resistance is mobilized after the beam deflects into the ground 0.5 in for granular soils and 1.0 in for fine-grained soils. The minimum resistance is reached after the beam moves out 0.05 in for granular soils and 0.2 in for fine-grained soils. Ground anchors were modeled as concentrated $T$-$y$ curves (anchor springs), where $T$ is the anchor load and $y$ is the deflection of the wall at the anchor location.

The trapezoidal apparent earth pressure diagrams presented in Section 2.1.5 include the effects of soil arching, stressing the ground anchors, the construction sequence, and the redistribution of earth pressures that occur on flexible walls in granular soils and stiff clays. They also consider the locations of the supports. Using these diagrams eliminated the need to analyze the wall for different construction stages. In the analysis the wall is "wished" into place.

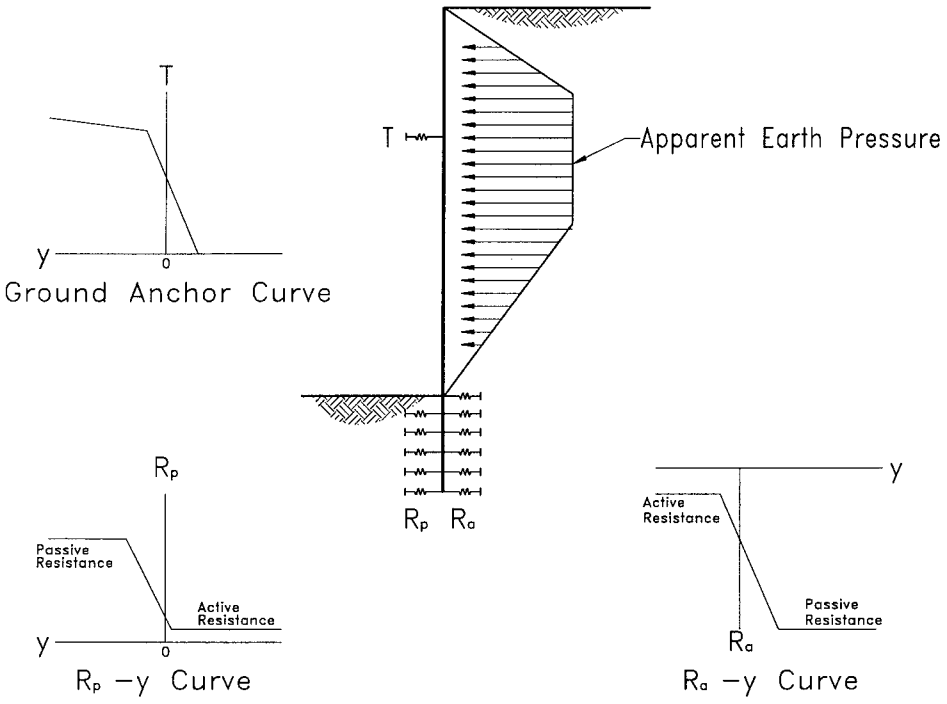


**FIGURE 30**
**Diagram Illustrating the Modeling of Earth Pressures, Toe Resistance, and Ground Anchors in a Soil-structure Interaction Analyses**

### 2.4.1 Predicted and Measured Bending Moments for a One-tier Wall

Soil-structure interaction analyses were performed on a 25-ft-high, one-tier wall constructed in a medium-dense sand having a friction angle of 32° and a total unit weight of 115 pcf. Soldier beams in the wall were HP10×57 sections located on 8-ft centers. A ground anchor, located 9 ft from the top of the beam and a 5-ft toe embedment supported the wall. Analyses using apparent earth pressures given by the 25*H* trapezoid (design diagram) and the modified trapezoidal diagram shown in Figure 6 were performed. The lateral resistance of the embedded portion of the soldier beams was modeled using *R-y* curves. The maximum resistances in each *R-y* curve are determined using the relationships in Section 2.2.2.

Figure 31 compares the bending moment diagrams from the soil-structure interaction analyses with the average bending moments measured in two instrumented soldier beams. Bending moment diagrams for the two trapezoidal diagrams assuming a hinge at the bottom of the excavation also are shown in Figure 31. The total lateral load for each apparent earth pressure diagram was 100 kips. The soldier beam in the soil-structure interaction analysis using the 25*H* trapezoid had to be lengthened 1 ft to obtain a solution. The 25*H* diagram requires the soldier beam toe to carry more load than the modified trapezoidal diagram. The soil-structure interaction analysis using the modified trapezoidal diagram predicted bending moments similar to those measured at the ground anchor location and larger than those measured in the span between the ground anchor and the bottom of the excavation. Bending moments determined using the modified trapezoidal apparent earth pressure and assuming a hinge at the bottom of the excavation fit the measured results the best.

### 2.4.2 Predicted and Measured Bending Moments for the Two-tier Wall

Soil-structure interaction analyses were performed on a 25-ft-high, two-tier wall constructed next to the one-tier wall (Section 2.4.1). Soldier beams in the wall were W6×25 sections located on 8-ft centers. The upper ground anchor was 6 ft from the top of the beam and the lower ground anchor was 10 ft below the upper anchor. Analyses using apparent earth pressures given by the 25*H* trapezoid (design diagram) and the modified trapezoidal diagram shown in Figure 6 were performed. The lateral resistance of the embedded portion of the soldier beams was modeled using *R-y* curves.

Figure 32 compares the bending moment diagrams from the soil-structure interaction analyses with the average bending moments measured in two instrumented soldier beams. Bending moments for the trapezoidal diagrams assuming a hinge at the lower ground anchor and the bottom of the excavation also are shown. The total lateral load for each apparent earth pressure diagram was 100 kips. Figure 32 shows that the soil-structure interaction analyses modeled the soldier beam as a continuous structural member and that the maximum predicted bending moments occurred at the ground anchor locations. The soil-structure interaction analysis using the modified trapezoid predicted the bending moments satisfactorily at the upper ground anchor location and below the lower ground anchor. Predicted moments between the ground anchors and at the lower anchor were higher than the measured bending moments. The maxi-

mum bending moments predicted by the design diagram and the maximum moment predicted by the soil-structure interaction analysis using the modified apparent earth pressure diagram were the same.

### 2.4.3 Observations

**Soil-structure interaction analyses using apparent earth pressure diagrams above the bottom of the excavation and *R-y* curves to model the lateral resistance of the soldier beam toe predicted the bending behavior of the walls satisfactorily. A soldier beam section and the toe embedment depth must be selected for a soil-structure interaction analysis. Apparent earth pressure diagrams include the effects of arching, soldier beam flexibility, pre-loading of the supports, facial stiffness, and the construction sequence.**

Figures 31 and 32 show that soldier beam bending moments can be predicted satisfactorily using the trapezoidal apparent earth pressure diagrams in Figure 6 with a hinge at subgrade. Bending moments at the upper ground anchor must be the same for the hinge method and the soil-structure interaction analysis. Below the upper ground anchor, the maximum bending moments computed using the hinge method were similar to the maximum bending moments predicted by the soil-structure interaction analysis. **For anchored walls with competent ground at subgrade, performing a soil-structure interaction analysis to determine the anchor loads and design moments is unnecessary. Apparent earth pressure methods can be done quickly and they do not require the selection of a structural section or toe embedment depth.** A soil-structure interaction analysis can be used to determine the bending moments when the designer wants to model the wall as a continuous member or when lateral toe resistance is low and the wall must cantilever around the lowest ground anchor.

**Wall deformations computed using soil-structure interaction analyses are not reliable.** The computed deformations do not include movements resulting from wall settlement, mass movements, and anchor yielding.

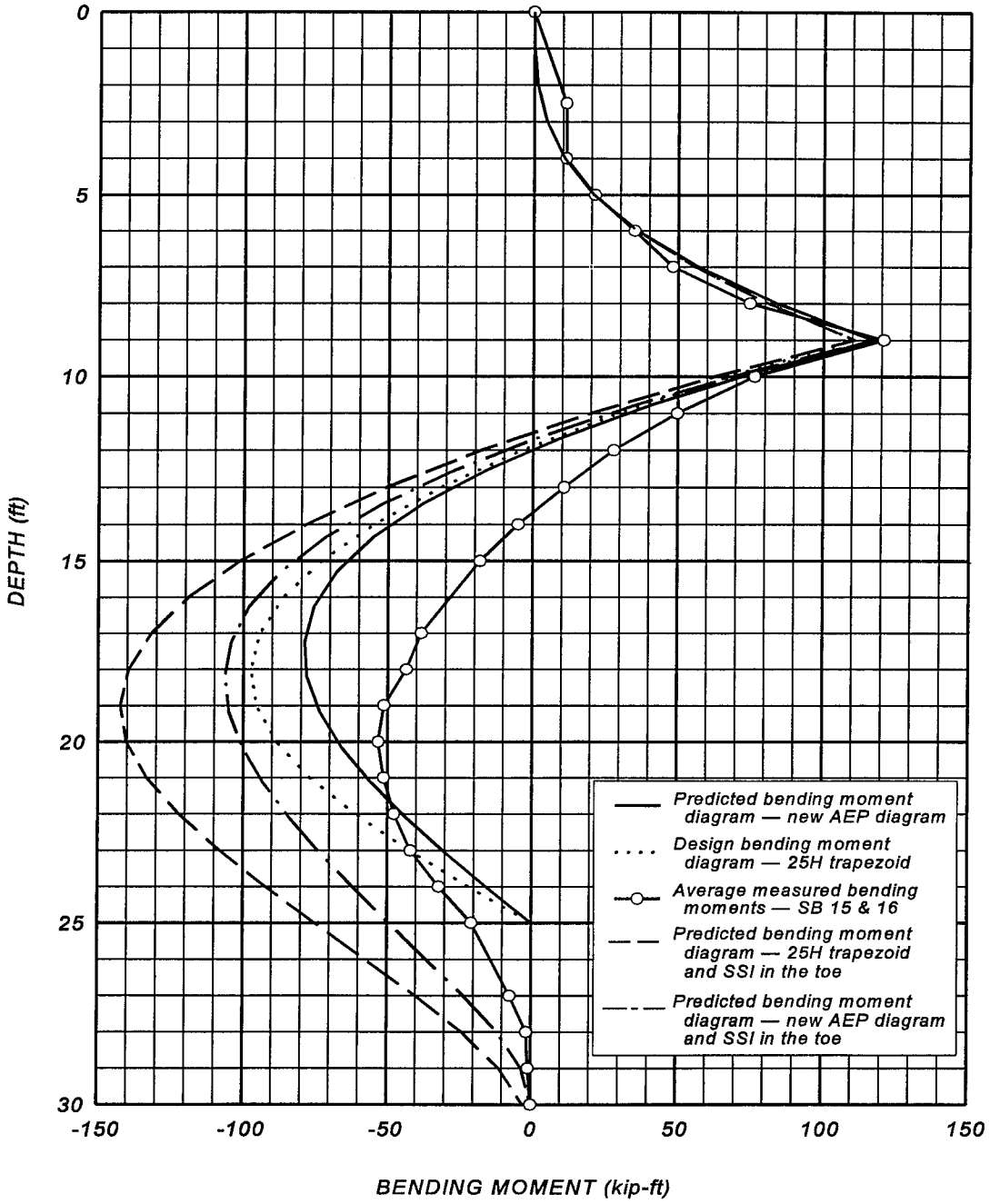


**FIGURE 31**
**Comparison of Predicted Bending Moments Using Trapezoidal Apparent Earth Pressure Diagrams and *R-y* Curves with Predicted Bending Moments Using Trapezoidal Apparent Earth Pressure Diagrams Assuming a Hinge at the Bottom of the Excavation and the Average Measured Bending Moments in Soldier Beams Installed in a One-tier Wall**

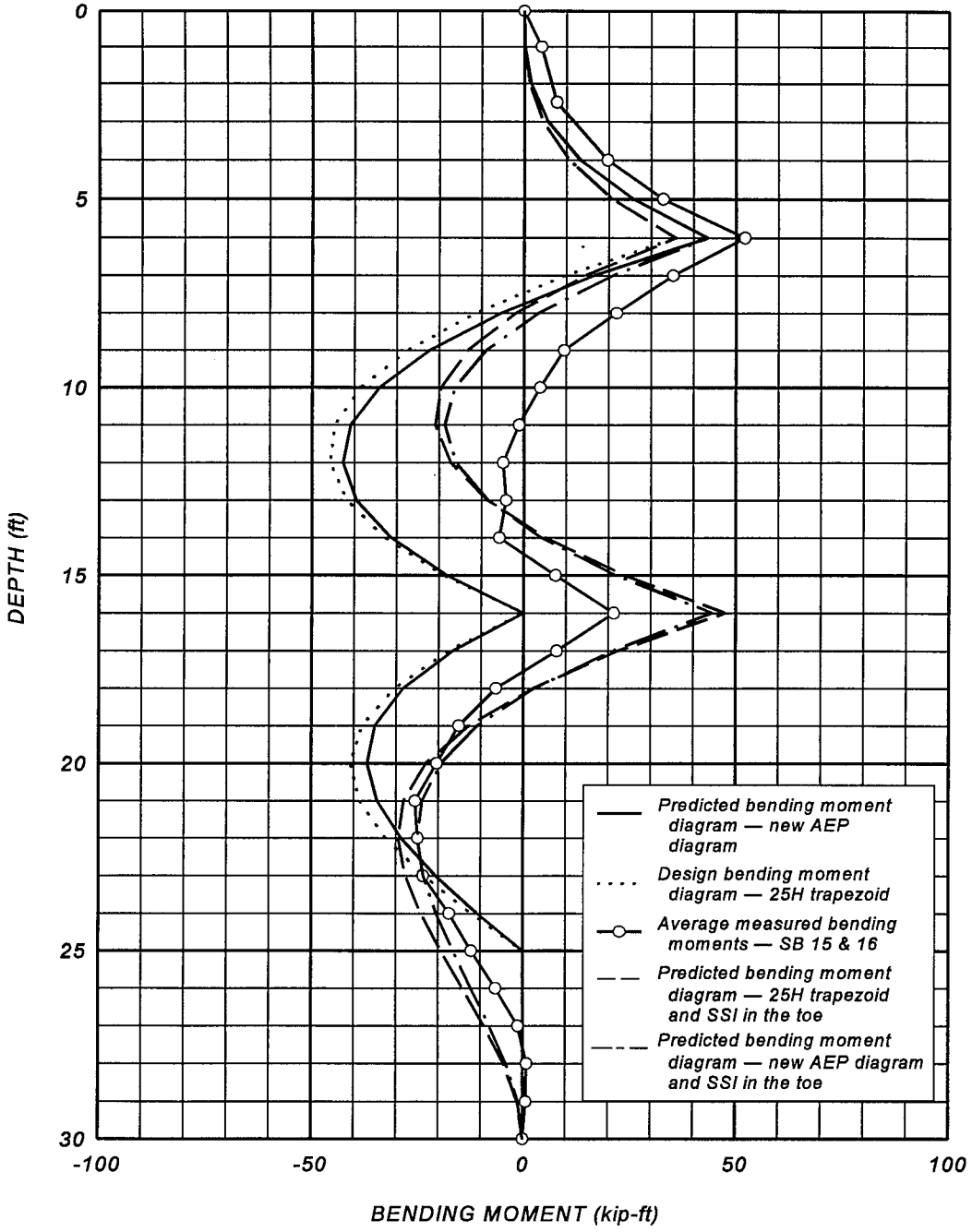


**FIGURE 32**
**Comparison of Predicted Bending Moments Using Trapezoidal Apparent Earth Pressure Diagrams and *R-y* Curves with Predicted Bending Moments Using Trapezoidal Apparent Earth Pressure Diagrams Assuming a Hinge at the Bottom of the Excavation and the Average Measured Bending Moments in Soldier Beams Installed in a Two-tier Wall Section**

## 2.5 WALL STABILITY

**Ground anchor walls must be internally and externally stable. Internal stability requires the ground anchors to be located sufficiently behind the wall so that the anchor does not develop load-carrying capacity from the ground supported by the wall. A wall is internally stable when any failure surface that passes between the wall and the top of the anchor bond length has an adequate factor of safety with the anchor load applied. External stability is satisfied if the ground anchors are long enough so that any failure surface that passes behind the back of the anchor bond zone has an adequate factor of safety. Internal and external stability is illustrated in Figure 33.**

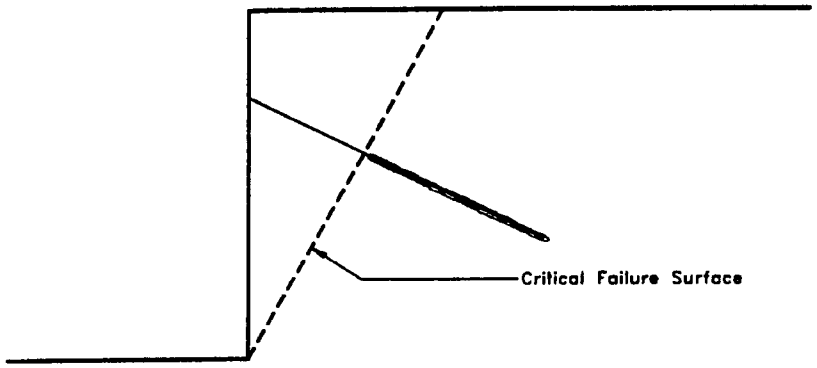


a) Internally stable wall (anchor bond length located behind the critical failure surface)

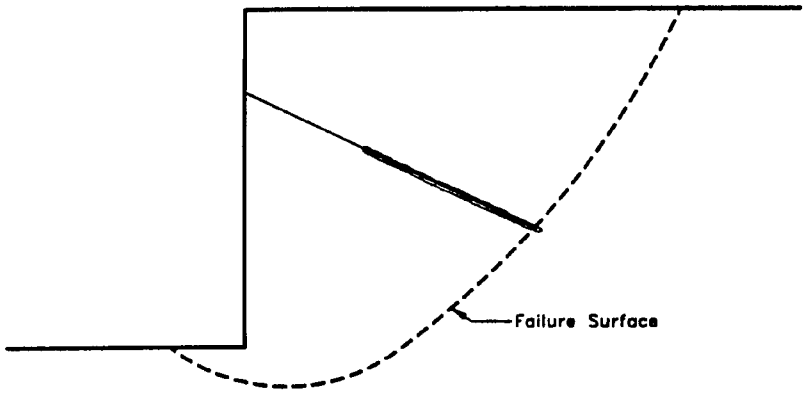


b) Externally stable wall (anchor extends to or beyond failure surface with adequate *FS*)

**FIGURE 33**
**Diagram Illustrating Internal and External Stability of an Anchor Wall**

On most projects it is only necessary to check the internal and external stability of the wall at one or two critical sections. These sections typically are the highest wall sections.

Figure 34 can be used to check the internal and external stability of walls with horizontal back slopes in granular soils. To use Figure 34, plot the ground anchor to scale and select a total anchor length that extends beyond the external stability curve appropriate for the soil at the site. Then check to ensure that the anchor bond length lies behind the critical failure surface. Lengthen the anchor if the anchor bond length is not adequate to develop the required ground anchor load-carrying capacity. Using Figure 34 will provide a factor of safety against an external stability failure of 1.3. Similar plots can be created for different factors of safety or sloping back slopes.

**When deep deposits of soft to medium clay exist below the bottom of the cut, the external stability failure surfaces may extend far below and behind the wall. When this occurs, usually the ground anchors are installed at a steep angle and anchored in good ground below the poor soils.**

External stability analyses assume that the ground anchors will develop load-carrying capacity uniformly along bond length. In most ground this is a reasonable assumption. However, **in ground that becomes much weaker with depth, the ground anchors may develop most of their load-carrying capacity near the front of the anchor bond length. These anchors may test satisfactorily, but not satisfy external stability.** In this type of ground, extend the unbonded length into the anchor bond length, and transfer the load to the back of the anchor first. When weak soil underlies good ground and the anchor will develop load-carrying capacity from both layers, design the ground anchors assuming that they will develop their capacity in the poorer soil.

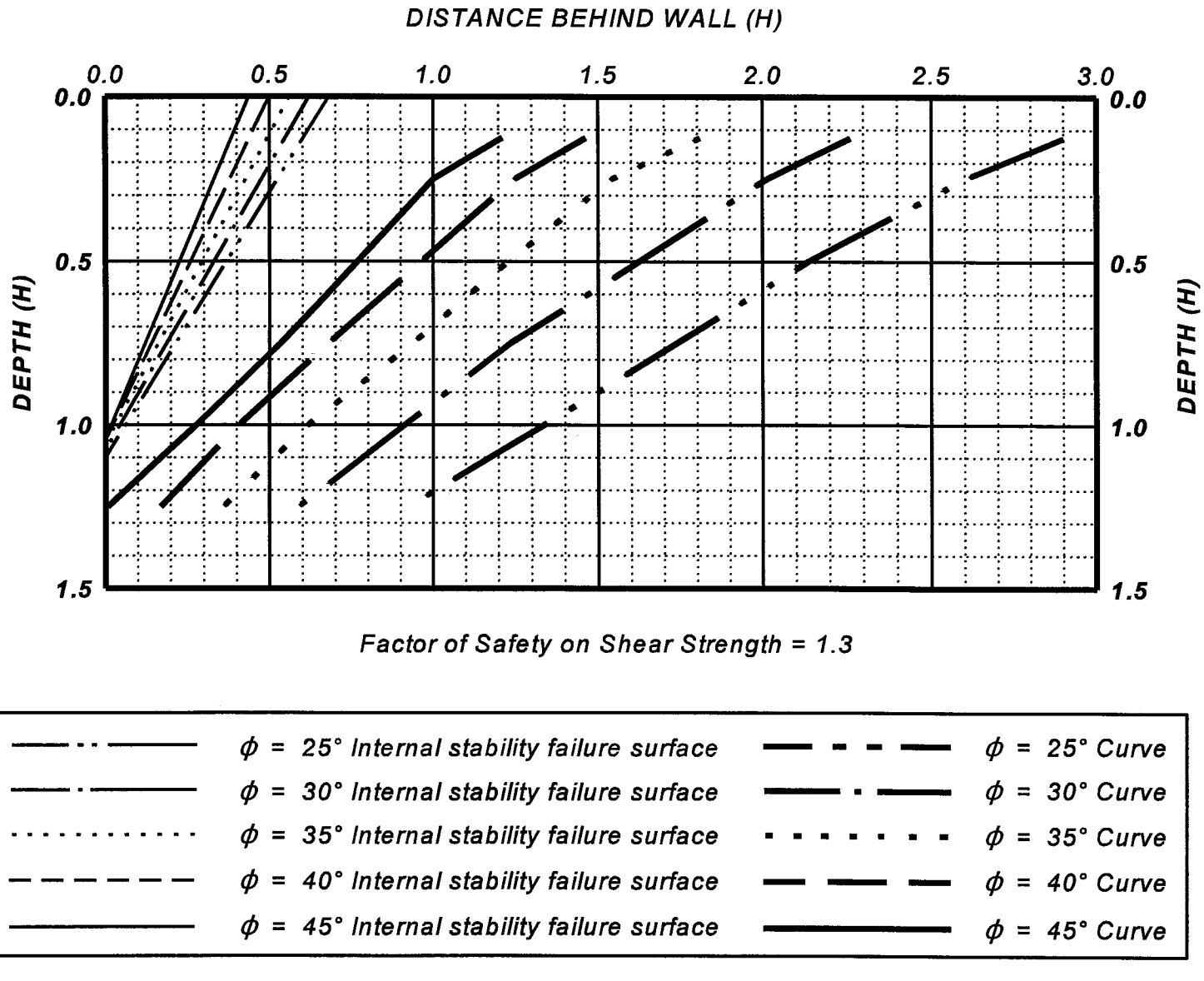


**FIGURE 34**
**Internal and External Stability Curves for Granular Soils (Scale: 2 in = *H*)**

## 2.6 WALL AND GROUND MOVEMENTS

**Lateral wall movements and ground surface settlements behind permanent ground anchor walls will be small.** These walls will be constructed in competent ground, and structures will not be nearby. **Typically, the maximum lateral wall movements will be about $0.002H$, and maximum vertical soil settlements will be about $0.0015H$, where $H$ is the height of the wall.**

**Lateral movements can result from bending deformations (cantilever movements and lateral bulging), outward rotation about the toe of the wall, and translation of the wall.** Settlement behind the wall is a response to the lateral wall movements or consolidation resulting from lowering the groundwater table. Bending deformations depend upon the height of the wall, stiffness of the wall, the distance to the first anchor, the distance between anchor levels, and the strength of the ground. Outward rotation about the toe is directly related to soldier beam settlement. Translation movements may result from mass movements behind the anchors, redistribution of load along the anchor bond length, anchor yielding, or elastic elongation of the anchor tendon in response to load increases. **In a well-designed wall, most of the deformation will be a result of bending deformations.** Rotational and translational movements will be small, with rotational movements larger than translational movements.

Wall and ground movements estimates are based on experience. Typical lateral and horizontal movements for flexible retaining walls have been presented by Peck (1969), Goldberg, et al. (1976), and Clough and O'Rourke (1990). Maximum lateral movements in ground suitable for permanent ground anchor walls are generally less than $0.005H$, with average maximum movements about $0.002H$. The largest lateral movement occurs at the top of the wall. Maximum vertical soil settlements in ground suitable for permanent ground anchor walls are less than $0.005H$, with average maximum settlement tending toward $0.0015H$. The maximum settlement occurs near the wall. For a 25-ft-high wall, a maximum lateral movement of 0.6 in and a maximum vertical ground settlement of 0.45 in would represent average performance.

**Lateral wall movements and ground settlements cannot be eliminated, but they can be reduced by controlling bending deformations and soldier beam settlements. Reducing the distance to the upper ground anchor will reduce the cantilever bending deformations, and reducing the span between the ground anchors will reduce the bulging deformations.** For flexible walls, the cantilever and bulging deformations can be expressed by Equations 2.24 and 2.25. These relationships were developed by Mueller, et al. (1998).

$$y_c = 4K_o\gamma h_1^2 / E_s \qquad \ldots [2.24]$$

$$y_b = 0.8K_o\gamma hL / E_s \qquad \ldots [2.25]$$

where:

$y_c$ = cantilever deformation

$y_b$ = bulging deformations

$K_o$ = at-rest earth pressure coefficient

$\gamma$ = total unit weight

$h_1$ = depth of excavation to allow the installation of the upper ground anchor

$E_s$ = represents a secant modulus on the soil's stress-strain curve (seeTable 8)

$h$ = depth of excavation

$L$ = span distance

**TABLE 8**
**Ranges for $E_s$ for Different Soil Types**

| SOIL | | $E_s$ (psi) |
|---|---|---|
| Clay | Firm to Stiff | 550 - 1150 |
| | Very Stiff | 1150 - 2850 |
| Silt | | 250 - 2850 |
| Loess | | 2150 - 8550 |
| Fine Sand | Loose | 1150 - 1700 |
| | Medium-dense | 1700 - 2850 |
| | Dense | 2850 - 4250 |
| Sand | Loose | 1400 - 4250 |
| | Medium-dense | 4250 - 7100 |
| | Dense | 7100 - 11400 |
| Gravel | Loose | 4250 - 11400 |
| | Medium-dense | 11400 - 14200 |
| | Dense | 14200 - 28450 |

The relationships given by Equations 2.24 and 2.25 are for soldier beam walls. When a stiff wall is used, the relationships are not valid. Movements estimated from the equations show trends, and they can be used to evaluate the impact of different ground anchor locations. They represent minimum movements that could be expected. They suggest that cantilever movement varies with the square of the depth of excavation, and bulging deformations are directly related to the distance between the ground anchors or the distance from the lower ground anchor to the bottom of the excavation. For a typical soldier beam wall, where $K_o$ = 0.4, $\gamma$ = 115 pcf, $h_1$ = 9 ft, $h$ = 25 ft, $L$ = 16 ft, and $E_s$ = 6000 psi the cantilever deformations equal 0.250 in and the bulging deformations equal 0.204 in.

**Controlling soldier beam settlements will limit lateral deformations of the wall. Installing ground anchors at flat angles will reduce the downward load applied to the soldier beams**

**and prevent soldier beam settlement.** Figure 35 shows how a steep anchor can cause soldier beam settlement and rotation of the wall around the toe.

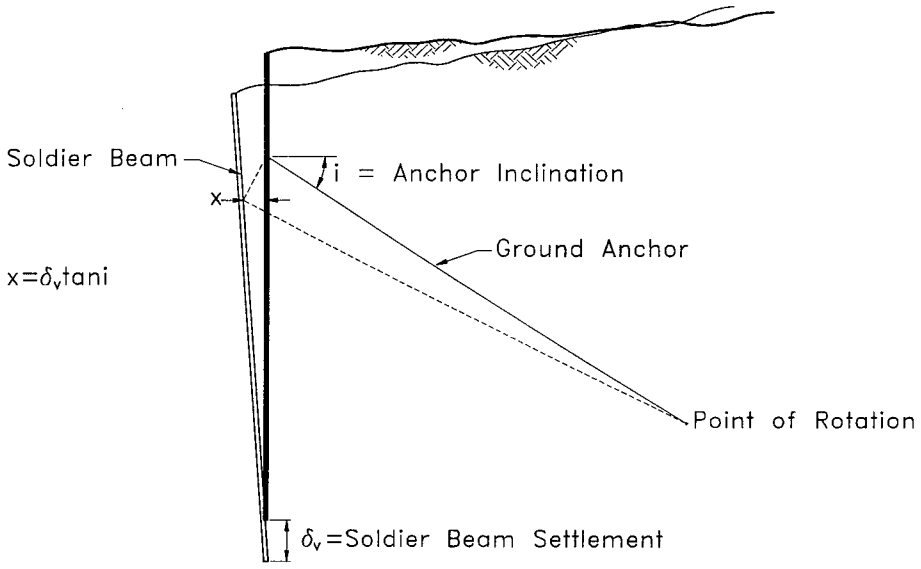


**FIGURE 35**
**Relationship Between Soldier Beam Settlement and Wall Movements**

**Practically, lateral movements and vertical settlements for most soldier beam walls cannot be reduced below 0.001*H*.**

## 2.7 CORROSION PROTECTION FOR ANCHOR TENDONS

Ground anchor tendon corrosion protection must be designed and constructed to ensure that the ground anchor will reliably support the wall for its design life. **Anchor tendons are fabricated using high-strength prestressing steels that are susceptible to embrittlement types of corrosion. When high-strength steels are used, the corrosion protection systems must be designed to prevent corrosion. Estimating design life by predicting metal loss is not valid for prestressing steels.** The Post-Tensioning Institute (PTI) (1996) shows that two classes of corrosion protection are used in the United States. Figure 36 shows a Class I Protection—Encapsulated Anchor Tendon, and Figure 37 shows a Class II Protection—Grout Protected Anchor. The unbonded length and anchorage area for both classes of protection assume that aggressive conditions exist near the structure. Similar protections are provided for the unbonded length and the anchorage of Class I and Class II protected anchors. Corrosion protections for the tendon bond lengths are different for the different classes of protection. Details about ground anchor corrosion protection can be found in American Association of State High-

way and Transportation Officials' (AASHTO) *The Standard Specifications for Highway Bridges* (1996), AASHTO-AGC-ARTBA Task Force 27 Report (1990), PTI's *Recommendations for Prestressed Rock and Soil Anchors* (1996), and *Tiebacks* (Weatherby, 1982).

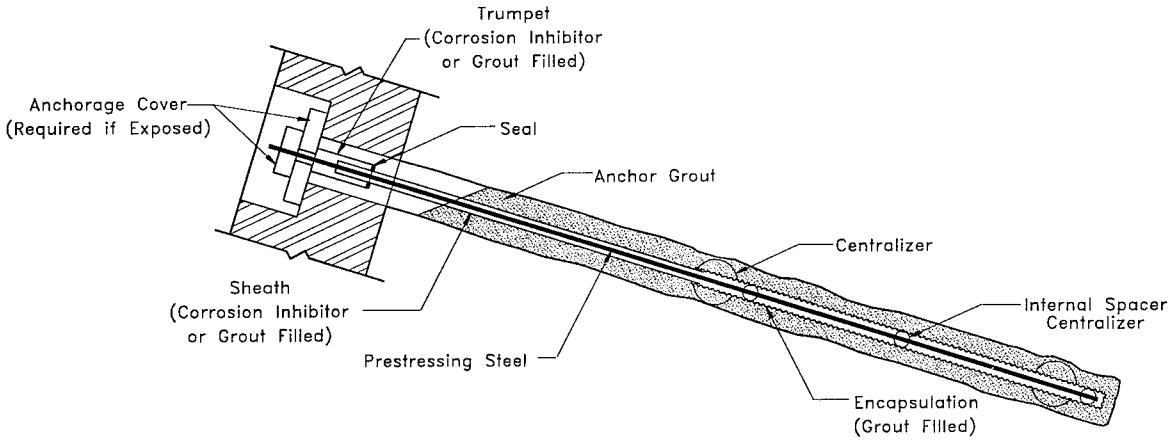


**FIGURE 36**
**Class I Protection—Encapsulated Anchor Tendon**

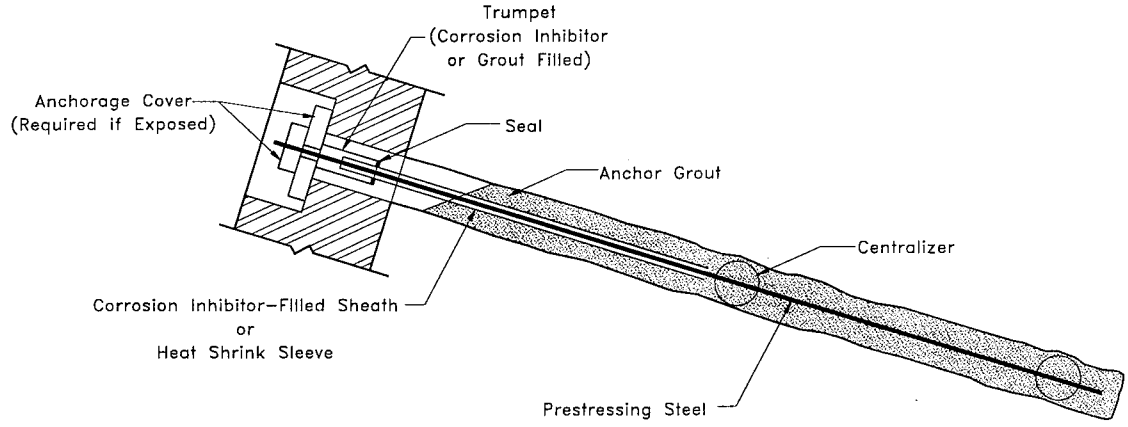


**FIGURE 37**
**Class II Protection—Grout Protected Anchor Tendon**

**Corrosion protection for the anchorage area is very important.** Most of the ground anchor tendon corrosion failures have occurred near the anchorage. The protection near the anchorage must be designed to protect the tendon where the corrosion protection over the unbonded length is terminated. A grout or corrosion inhibiting compound filled steel tube (trumpet)

attached to the bearing plate provides the protection for the prestressing steel just below the bearing plate. Most trumpets are filled with grout. If a corrosion inhibiting compound is used, then the seal between the trumpet and the unbonded length corrosion protection must function for the life of the structure. If grout is used to fill the trumpet, the seal between the tendon and the trumpet only has to function until the grout has set. The anchorage for most permanent ground anchor walls will be encased in the concrete. If the anchorage remains permanently exposed, it should be protected by a grout or a corrosion inhibiting compound filled cover. Grout should be used if possible. **Good detailing, care during construction, and inspection are necessary to ensure that the anchorage protection is done properly.**

Figure 38 shows that the class of corrosion protection system for a permanent ground anchor is based on aggressivity, consequences of tendon failure, and an evaluation of the extra costs for installing an encapsulated tendon versus the benefits of having the encapsulation.

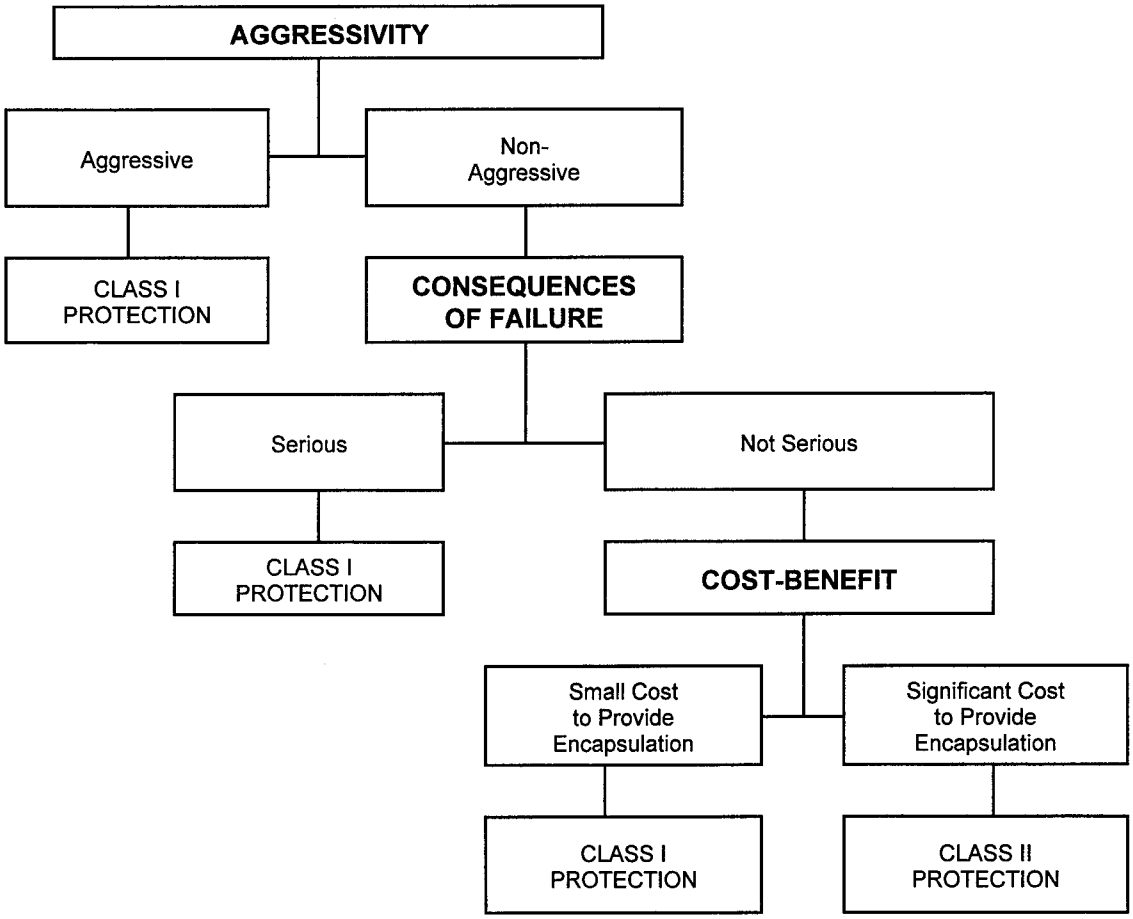


**FIGURE 38**
**A Guide for Selecting the Class of Corrosion Protection for a Ground Anchor Tendon**

**Ground is considered aggressive if it has one or more of the following: a pH value less than 4.5, a resistivity less than 2000 ohm-cm, sulfides present, stray currents present, or caused chemical attack to other buried concrete structures.** The ground is assumed to be aggressive if aggressivity tests are not done. Salt water or tidal marshes, cinder fills, ash or slag fills, organic fills containing humic acid, peat bogs, acid mine wastes, or industrial wastes are considered aggressive ground.

If the corrosion failure of a single ground anchor tendon could result in serious consequences, then a Class I Protection is recommended. A single anchor tendon failure will not have a serious impact on the performance of a permanent ground anchor wall. Ground anchor walls will redistribute load if an anchor tendon fails. To verify this, load was reduced on two ground anchors as part of the research reported by Weatherby, et al. (1998). After the load reduction the wall was monitored for 1 year. The reduction in load had little effect on the adjacent ground anchors and soldier beam moments. (Adjacent ground anchors were locked-off at a load equal to 75 percent of their design load.) Broms (1988) reported similar results on temporary excavation support systems in weak cohesive soils.

The final criterion for selecting the class of corrosion protection is the incremental cost for changing from a Class II Protection to a Class I Protection. The cost to provide an encapsulated tendon can be more than just the costs of the protection. Encapsulating the tendon bond length increases the diameter of the tendon, and may require a more expensive installation method than one suitable for a Class II Protection. In an open drill hole, the cost difference can be small, and the designer may elect to use a Class I Protection even though one is not necessary. If the cost of switching from a Class II Protection to a Class I Protection is significant, then the designer may determine that the benefit of encapsulating the tendon is not worth the additional costs associated with a Class I Protection.

## 2.8 CORROSION PROTECTION FOR SOLDIER BEAMS

Soldier beam corrosion problems have not been reported. Soldier beams are fabricated from Grade 36 or Grade 50 structural steels. These steels are not subject to embrittlement corrosion like the prestressing steel used to fabricate the ground anchor tendon. If corrosion develops on a soldier beam, it will be distributed over a portion of the surface or localized in a pit. Both types of corrosion cause a loss of section, but they do not cause dramatic failure of the member. Unless the environment is acidic, pH less than 4, oxygen must be present and the ground must be a good electrolyte for corrosion to continue in the underground. Romanoff (1962 and 1969) presented the results of National Bureau of Standards studies on the corrosion of driven steel piles. Soil conditions at the sites varied widely, from well-drained sands to clays. The resistivity of the soils ranged from 300 ohm-cm to 50,200 ohm-cm and the pH ranged from 2.3 to 8.6. **Romanoff found that the steel pilings were not affected by corrosion in undisturbed natural soils regardless of the soil types or properties. He found minor to moderate corrosion in the form of shallow pits on piles driven through fills or in soils above the**

**groundwater table. The average reduction in wall thickness on any of the piles examined was not significant enough to impair the useful life of the structure.**

**Corrosion is not a concern for drilled-in soldier beams.** Drilled-in soldier beams are surrounded either by lean-mix backfill or structural concrete. Lean-mix backfill and structural concrete create a high pH environment for the steel soldier beam. In a high pH environment, a diffusion barrier of hydrous ferrous oxide will develop on the surface of the steel. This barrier will prevent oxygen from reaching the surface of steel and keep the rate of corrosion very low.

**If buried concrete structures in the vicinity suffer from attack, then drilled-in soldier beams should be coated. Galvanizing, coal-tar epoxy coatings, or fusion-bonded epoxy coatings are suitable.**

Recent observations of corrosion on driven foundation piles in natural ground have led FHWA to recommend evaluating the corrosion of driven steel soldier beams in accordance with National Cooperative Highway Research Program (NCHRP) 10-46 when published or AASHTO *Standard of Recommended Practice* when approved. In the interim before these guidelines are available, if fill soils are present in locations where the driven soldier beam bending moments are expected to be high, the beams should be protected from corrosion. Corrosion protection can consist of increasing the thickness of the member to account for section loss or applying a coating. Increasing the thickness of the flange and web by 1/16 of an inch will allow for a metal loss of 1.25 mils/year for 50 years. Instead of increasing web and flange thickness, higher strength steels can be used at lower allowable strengths (using Grade 50 steel at Grade 36 steel allowable stresses would allow a 39 percent loss in section). When the pH is less than 4, the soldier beams should be coated or drilled-in. Coal tar epoxy or fusion-bonded epoxy coatings are recommended.

## 2.9 GROUND ANCHORS

### 2.9.1 Large-diameter Ground Anchor Tests

Ten, 12-in-diameter, hollow-stem-augered tiedown anchors were load tested as part of the ground anchor wall research. Six of the anchors were instrumented to allow the strains in the anchor grout and the tendon to be measured. Four of the anchors were loaded and monitored for 70 days. The results of the test program are:

- **Large-diameter, hollow-stem-augered anchors develop load-carrying capacity along the grout shaft surrounding the unbonded tendon length.**
- **Recommend developing a "compression" anchor by extending the unbonded tendon length to at least the mid-point of the anchor bond length.**

- **Compression anchors develop their load-carrying capacity from the lower portion of the anchor, and prevent the development of significant load-carrying capacity in the "no-load" zone.**
- **Compression anchors can be grouted to the ground surface in one phase.**
- Compression anchors are axially stiffer than anchors with tendon bond lengths equal to the anchor bond length.
- Higher grout to soil bond stresses are developed along the grout shafts of stiff anchors than along the shafts of more flexible anchors.
- Stiff anchors develop higher ultimate loads than flexible anchors with the same bond lengths.
- **Short-term creep testing satisfactorily evaluated the long-term load-carrying capacity of ground anchors installed in fine-grained soils. Creep movements and load losses predicted from short-term tests were similar to values measured during a 70-day load hold.**
- **Anchor acceptance criterion of 0.08 in of creep movement per decade of time is valid for large-diameter, hollow-stem-augered anchors.**
- **Retesting of low-pressure grouted anchors installed in fine-grained soils should not be allowed. Preloading during initial testing will affect the test results during re-testing. Creep movements will be significantly less during the second test.**
- **Regroutable anchors in fine-grained soils may be retested. Retesting procedures must consider the effects of pre-loading on the creep movements measured during retesting.**

### 2.9.2 Unbonded and Tendon Bond Lengths for Small-diameter Ground Anchors

**The tendon bond length and the anchor bond length coincide for high-pressure grouted anchors, small-diameter anchors, and rock anchors. The unbonded tendon length is selected so the anchor bond length is behind the critical failure surface.**

### 2.9.3 Ground Anchor Lock-off Load

**Ground anchors are usually prestressed to between 75 and 100 percent of their design load. Anchor loads normally do not increase significantly after lock-off. The loads do not increase because the lock-off loads and the lateral toe resistance provide a resultant thrust between the Rankine and the at-rest load. Full-scale and model-scale wall tests suggest that lock-off loads equal to 75 or 80 percent of the design load are desirable.** Increasing the lock-off loads above 80 percent of the design load will result in higher soldier beam bending moments at the ground anchors and larger axial loads in the soldier beams.

### 2.9.4 Ground Anchor Load Reduction

Visual observations and measurements showed that the wall remained serviceable after the load on two ground anchors supporting the full-scale wall was reduced. Lateral wall movements increased in response to reducing the load. Bending moments decreased in the soldier beams supported by the ground anchors whose load was reduced. Bending moments in adjacent soldier beams remained essentially unchanged as the load was reduced. Bending moment changes would not require the soldier beam to be redesigned. Bending moment, lateral wall movement, and ground anchor load changes in response to unloading the two ground anchors show that the wall would be serviceable if an anchor failed to carry the design load.

## 2.10 STRAIN GAUGE ERRORS

Welding to attach wood lagging boards to the soldier beams caused compression strains on the front flanges of the instrumented soldier beams. Avoid welding on instrumented beams after the strain gauges are zeroed. If welding must be done, read all strain gauges before and after welding to detect the effect of welding and correct the reading for the strains induced by the welding operation. Wait 24 hours after the welding is complete to take the second set of readings. No construction activities should occur before the second set of readings are obtained.

## 2.11 COMPOSITE BEHAVIOR OF DRILLED-IN SOLDIER BEAMS

**Composite behavior did not exist where the drilled-in soldier beams in the full-scale test wall were backfilled with lean mix fill. Where lean mix fill is used, design procedures should assume that all the load is carried by the steel section. The steel beam and the structural concrete in the toes of the soldier beams of the full-scale wall may have behaved as a composite near the bottom of the toes.** Assuming that the load is carried by the steel soldier beam is conservative if structural concrete is used to backfill the drilled shaft.

**Satisfactory behavior was obtained when the toe was backfilled with lean mix fill. When lean mix is used to backfill around the toe, compute the axial load-carrying capacity assuming the steel section punches through the lean mix, and the capacity based on drilled-shaft relationships. When selecting a toe depth, use the smaller capacity. Use the width of the steel soldier beam when determining the lateral toe resistance for drilled-in soldier beams backfilled with lean mix.**

## 2.12 CONSTRUCTIBLE DESIGNS

**A constructible design requires an understanding of the interrelationship between the different components of a ground anchor wall. The design must be flexible and allow for replacement anchors if failures are expected.** On most projects, ground anchor failures rates are less than 1 to 2 percent. Most anchor failures occur at the beginning of a project, or in low-strength ground, or when ground conditions change. Speciality contractors, who design and build anchored walls, understand how the different components of an anchored wall fit

together. **To obtain a constructible wall at the best price, the contract documents should clearly establish the design requirements and require the contractor to prepare detailed design drawings. The contractor should select the soldier beam type and installation method, ground anchor type and load-carrying capacity, connection details, and facing type.**

# CHAPTER 3
# RESEARCH NEEDS

During the performance of the research and the preparation of the final report and the design manual, several research needs emerged. These research needs are presented in this chapter.

## 3.1 WALL MOVEMENTS AND GROUND DEFORMATIONS

Current permanent ground anchor wall design procedures focus on determining anchor loads and bending moments in the wall. Lateral wall movements and vertical settlements are not predicted but they are expected to be less than $0.002H$ and $0.0015H$, respectively. When the designer is concerned about ground movements behind the wall, the earth pressures are increased and a stiff wall is used. These walls are expensive. At some sites, nearby structures are underpinned or supported by a means independent from the wall.

Research performed under this contract identified three types of wall movements. They are bending deformations, rotational movements, and translational movements. Today, we understand the causes of these movements, but we have not developed the ability to predict them accurately. Bending deformations can be controlled by selecting anchor spacings and wall stiffness. Rotational movements can be eliminated by selecting flat ground anchor angles and building a wall with adequate axial load-carrying capacity. Translational movements can be controlled by ensuring that the ground anchors will not experience large time-dependent movements (creep), and that the wall is externally stable.

Careful monitoring of walls will allow the three components of wall movements to be measured. Then relationships to predict wall and ground movements from each component of movement can be developed. When reliable deformation predictions can be made, design procedures that include ground movement criteria should be developed. In crowded cities, the ability to predict wall and ground movements will allow the most economical walls to be built and reduce the damage to adjacent structures.

## 3.2 STIFF CLAYS

AASHTO (1996) requires that permanent ground anchor walls in stiff clay be designed to support earth pressures determined from the stiff clay apparent earth pressure diagram and an effective stress analysis. The drained friction angle used in an effective stress analysis is often the drained friction angle for the clay in its normally consolidated state. Drained friction angles between 20° and 30° are common. Most of these clay deposits are overconsolidated and their long-term, drained friction angles may be higher than the values used in design. Research directed toward determining the drained shear strength for permanent ground anchor walls has the potential of reducing the earth pressures on many walls by up to 35 percent.

Volume changes and the availability of porewater are necessary for an overconsolidated clay to experience a significant strength loss. Research directed toward preventing or controlling the loss of strength in a stiff clay behind a wall may develop techniques that can be used on sites with overconsolidated fine-grained soils. For example, large-diameter, hollow-stem-augered anchors grouted over their full length may act as reinforcements and resist the volume changes that are necessary for the strength loss to occur.

Design rules for determining the "no-load" zone (critical failure surface) and the total anchor lengths for ground anchors in stiff clay need to be verified or revised. Stability analyses are used to define the critical failure surface and the external stability failure surface for walls built in granular soils or soft to medium clays. Stability analyses using undrained shear strengths show that many walls in stiff clays are internally and externally stable without the ground anchors. Drained shear strength parameters can be used to check the internal and external stability of these walls, but a more fundamental understanding of the stability of walls in stiff clays is necessary. It is possible that short ground anchors can be used to support permanent ground walls constructed in intact, stiff clay deposits.

## 3.3 UNIFIED DESIGN FOR IN SITU WALLS

Ground anchor walls and soil nailing walls are built from the top down. A unified design approach based on limiting equilibrium methods can be developed for both wall types. A unified design approach would allow both wall types to have similar factors of safety. The procedure would help the designer to develop a fundamental understanding of both walls and could guide the designer to select the best wall system for each project.

## 3.4 SOLDIER BEAMLESS WALLS

In competent ground, permanent ground anchor walls can be built using horizontal beams to distribute the ground anchor load to the ground. The horizontal beams are constructed as the excavation is made and no soldier beams are installed. This type of wall has been built along highways in mountainous regions for roadway realignment or to stabilize a landslide. Monitoring and documenting the performance of soldier beamless walls will encourage highway departments to use them. When soldier beam installation is very expensive, these walls offer substantial cost savings if the ground between the horizontal beams requires little support or is self supporting.

## 3.5 TEMPORARY EXCAVATION SUPPORT SYSTEMS

Geotechnical engineers do not agree how to determine the shear strength for the design of temporary excavation support systems in deep deposits of soft to medium clay. Strengths determined using laboratory tests have not been reliable in predicting the performance of some of

these systems. Unfortunately, many contract plans and specifications present only the laboratory test results and provide no guidance for selecting the shear strengths to be used in design. Developing tests or relationships to estimate the strength for design would avoid performance problems, conflicts, claims, and construction delays.

Occasionally temporary excavation support systems are constructed in ground where competent ground overlies a deep deposit of weak ground. Ground anchors supporting a wall in this type of profile may develop their load-carrying capacity in the competent ground and satisfy the load testing acceptance criteria. The external stability of these walls may not be adequate, since current external stability guidelines assume that the anchors uniformly develop load-carrying capacity along the anchor bond length and force external stability failure surfaces to extend behind the ground anchors. A combination of analytical studies and monitoring of excavation support systems in this type of profile need to be undertaken to develop guidelines for evaluating the external stability of these temporary excavation support systems.

Three-in-thick lagging boards, or a lightly reinforced shotcrete layer are used to temporarily support the ground between the soldier beams. These two means of supporting the ground have worked well. Some agencies require the temporary support to be designed for the full earth pressures applied to the wall. When the temporary support is designed, it becomes much thicker and more expensive than the wood lagging that has worked for more than 100 years. Using thick lagging boards (up to 8 in) is a waste of our natural resources. If highway departments want to require that the lagging boards be designed, then design relationships that explain how 3-in lagging works should be developed.

# CHAPTER 4
# IMPLEMENTING THE RESULTS OF THIS RESEARCH

AASHTO's *Standard Specification for Highway Bridges* should be revised to reflect the results of the research performed on this contract. Modification in the following areas would have a significant impact on the cost of permanent ground anchor walls:

- Design one-tier walls for apparent earth pressure diagrams.
- Assume a hinge in the soldier beam at the bottom of the excavation when computing soldier beam bending moments and anchor loads in granular soils, stiff clays, and soft to medium clays with competent ground at the bottom of the excavation.
- Assume the ground at the toe acts as a strut in granular soils, stiff clays, and soft to medium clays with competent ground at the bottom of the excavation.
- Compute the lateral toe resistance using laterally loaded pile relationships developed by Wang and Reese (1986).
- Design all soldier beam and sheet pile walls using apparent earth pressure diagrams and discontinue checking each stage of construction.
- Use 3-in-thick wood lagging to temporarily support the ground between soldier beams.
- Allow lean-mix fill to be used to backfill soldier beam toes.
- Encourage contractors/designers to be innovative in the development of their design rather than prescriptive.

Contracting agencies should develop and adopt a performance specification that encourages contractors to pick the best wall system for a particular location, and requires them to design and build that wall system. Design requirements in the specification should follow the *Design Manual for Permanent Ground Anchor Walls* (Weatherby, 1997). Contractors understand the interrelationship between each component of the wall and are best able to combine their capabilities and the different wall components into a buildable design. Less expensive walls and fewer claims will result when owners use a performance specification that requires the contractor to design and construct the walls.

# REFERENCES


AASHTO-AGC-ARTBA Joint Committee Task Force 27 Report (1990). *Specification for Permanent Ground Anchors*, Washington, DC.

AASHTO (1996). *The Standard Specification for Highway Bridges*, 16th Edition, Washington, DC.

Achilleos, E. (1988). *User Guide for PC STABL 5M*, Purdue University, West Lafayette, IN.

Bishop, A.W. (1955). "The Use of the Slip Circle in the Stability Analysis of Slopes," *Geotechnique*, Vol. 5, No. 1, pp. 7-17.

Broms, B.B. (1988). "Design and Construction of Anchored and Strutted Sheet Pile Walls in Soft Clay," *Proceedings 2nd International Conference on Case Histories in Geotechnical Engineering*, St. Louis, MI.

Clough, G.W. and O'Rouke, T.D. (1990). "Construction Induced Movement of In-situ Walls," *Proceedings ASCE Specialty Conference Design and Performance of Earth Retaining Structures*, Cornell Univ., Ithaca, NY.

Goldberg, D.T., Jaworski, W.E., and Gordon, M.D. (1976). *Lateral Support Systems and Underpinning*, Report No. FHWA-RD-75-128, Vol. 1, Federal Highway Administration, Washington, DC.

Henkel, David J. (1971). "The Calculation of Earth Pressures in Open Cuts in Soft Clays," *The Arup Journal*, Vol. 6, No. 4, pp. 14-15.

Janbu, N., Bjerrum, L., and Kjaernsli, B. (1956). "Soil Mechanics Applied to Some Engineering Problems," in Norwegian with English summary, *Norwegian Geotechnical Publication 16.*

Long, J.H., Weatherby, D.E., and Cording, E.J. (1998). *Summary Report of Research on Permanent Ground Anchor Walls*, "Volume I: Current Practice and Limiting Equilibrium Analyses," Report No. FHWA-RD-98-065, Federal Highway Administration, McLean, VA.

Mueller, C.G., Long, J.H., Weatherby, D.E., Cording, E.J., Powers III, W.F., and Briaud, J.-L. (1998). *Summary Report of Research on Permanent Ground Anchor Walls*, "Volume III: Model-scale Wall Tests and Ground Anchor Tests," Report No. FHWA-RD-98-067, Federal Highway Administration, McLean, VA.

## REFERENCES
*(continued)*


Navy, Department of (May 1982). *Foundations and Earth Structures*, NAVFAC DM-7.2. Available from Department of the Navy, Naval Facilities Engineering Command, 200 Stovall Street, Alexandria, VA 22332, p. 63.

Peck, R.B. (1969). "Deep Excavations and Tunneling in Soft Ground, State of Art Report," *7th ICSMFE*, Mexico City, pp. 225-290.

PTI (1996). *Recommendations for Prestressed Rock and Soil Anchors*, 3rd Edition, Post-Tensioning Institute, Phoenix, AZ.

Reese, L.C. (1958). Discussion of "Soil Modulus for Laterally Loaded Piles," by McClelland and Focht, *Transactions*, ASCE, Vol. 123, pp. 1071-1074.

Reese, L.C., Cox, W.R., and Koop, F.D. (1974). "Field Testing and Analysis of Laterally Loaded Piles in Sand," *Proceedings of the 5th Offshore Technology Conference*, Houston, Texas, Paper No. OTC 2080, Vol. II.

Romanoff, M (1962). *Corrosion of Steel Pilings in Soils*, National Bureau of Standards (U.S.) Monogram 58.

Romanoff, M (1969). "Performance of Steel Pilings in Soils," *Proceedings 25th Conference National Association of Corrosion Engineers*, p. 14.

Schnabel, Jr., H. (1982). *Tiebacks in Foundation Engineering and Construction*, McGraw-Hill Book Company, New York.

Terzaghi, K. and Peck, R.B. (1967). *Soil Mechanics in Engineering Practice*, John Wiley & Sons, New York.

Terzaghi, K., Peck, R.B., and Mesri, G. (1996). *Soil Mechanics in Engineering Practice*, 3rd Edition, John Wiley & Sons, New York.

Urzua, A. and Weatherby, D.E. (1998). *TB Wall - Anchored Wall Design and Analysis Program for Personal Computers*, Report No. FHWA-RD-98-093, Federal Highway Administration, McLean, VA.

Wang, S.-T. and Reese, L.C. (1986). *Study of Design Methods for Vertical Drilled Shaft Retaining Walls*, Texas State Department of Highways and Pubic Transportation, Austin, TX.

# REFERENCES
*(continued)*

Wang, S.-T. and Reese, L.C. (1992). *COM624P: Laterally Loaded Pile Analysis Program for the Microcomputer, Version 2.0*, FHWA Report No. SA-91-048, Washington, DC.

Weatherby, D.E. (1982). *Tiebacks*, Report No. FHWA Report No. RD-82/047, Federal Highway Administration, Washington, DC.

Weatherby, D.E. (1997). *Design Manual for Permanent Ground Anchor Walls*, Report No. FHWA-RD-98-130, Federal Highway Administration, McLean, VA.

Weatherby, D.E., Chung, M., Kim, N.-K., and Briaud, J.-L. (1998). *Summary Report of Research on Permanent Ground Anchor Walls*, "Volume II: Full-scale Wall Tests and a Soil-structure Interaction Model," Report No. FHWA-RD-98-066, Federal Highway Administration, McLean, VA.